

# Line outage distribution factors of a linearized AC model with reactive power and voltage magnitude for resilience-constrained economic dispatch



Zhaoxiong Huang<sup>a</sup>, Liping Huang<sup>a,\*</sup>, Chun Sing Lai<sup>a,b,\*\*</sup>, Youwei Jia<sup>c</sup>, Zhuoli Zhao<sup>a</sup>, Xuecong Li<sup>a</sup>, Loi Lei Lai<sup>a,\*</sup>

<sup>a</sup> Department of Electrical Engineering, School of Automation, Guangdong University of Technology, Guangzhou 510006, China

<sup>b</sup> Brunel Interdisciplinary Power Systems Research Centre, Department of Electronic and Electrical Engineering, Brunel University London, London, UB8 3PH, UK

<sup>c</sup> Department of Electrical and Electronic Engineering, Southern University of Science and Technology, Shenzhen, 518055, China

## ARTICLE INFO

### Article history:

Received 30 October 2021

Received in revised form 19 May 2022

Accepted 5 June 2022

Available online 11 June 2022

### Keywords:

Economic dispatch

Linearized AC power flow

Line outage distribution factor

Power system resilience

Sensitivity factors

## ABSTRACT

Research on preventive generation dispatch schemes for resilient power system operation is often based on the DC power flow model, ignoring the influence of reactive power and voltage magnitude. This paper presents an in-depth study of a linearized AC power flow (LAC) model with reactive power and voltage magnitude to derive sensitivity factors, including shift factors and line outage distribution factors, for pre-contingency and post-contingency power flow calculations for N-k contingencies. Based on the derived sensitivity factors, a resilience-constrained economic dispatch (LAC-RCED) strategy is developed, which considers the security constraints of N-1 contingency for all lines and N-2 contingency for the affected lines, as well as optimization objectives to improve the power flow distribution in the transmission system. To deal with the computational difficulties associated with the N-k contingency constraints, an iterative contingency filtering algorithm based on the derived line outage distribution factor is proposed for contingency screening and creating security constraints for violated contingency scenarios. In the case study, the accuracy of the power flow solution obtained from the derived sensitivity factors is investigated by comparison with the AC model. The proposed LAC-RCED model and the iterative contingency filtering algorithm are tested on the IEEE 30-bus and 118-bus systems.

© 2022 The Author(s). Published by Elsevier Ltd. This is an open access article under the CC BY license (<http://creativecommons.org/licenses/by/4.0/>).

## 1. Introduction

Due to climate change in recent years, the impact of extreme weather events on power systems has become increasingly evident. The resilience of the power system to these extreme events has attracted widespread attention [1,2]. Resilience enhancement strategies for transmission systems can be generally classified into planning-based and operation-based approaches [3]. Planning-based methods focus on developing network expansion strategies to strengthen the electricity infrastructure and avoid component failures in extreme events, whereas operation-based

approaches aim to utilize the available assets to develop resilient operation strategies. These strategies might provide preventive, corrective, or restorative approaches to cope with or mitigate the extreme event. This paper focuses on preventive resilient operations.

Several models and approaches have been proposed in the literature in the context of enhancing power system operational resilience [4–10]. Resilience-based unit commitment and economic dispatch strategy are one of the main approaches. In [4] an event-driven security-constrained unit commitment model was proposed by considering the simultaneous outages of multiple system components affected by a predicted hurricane. A sequentially proactive enhancement strategy was adopted to enhance the system resilience in [5]. Resilient operation strategies based on multi-level optimization problems are presented in [6–8]. Different from the above works, the optimization models proposed in [9,10] take into account optimization objectives related to power flow on transmission lines in addition to the generation cost. Numerical results demonstrate the effectiveness of the proposed model in preventing cascading overload outages caused by

\* Corresponding authors.

\*\* Corresponding author at: Brunel Interdisciplinary Power Systems Research Centre, Department of Electronic and Electrical Engineering, Brunel University London, London, UB8 3PH, UK.

E-mail addresses: [3115001026@mail2.gdut.edu](mailto:3115001026@mail2.gdut.edu) (Z. Huang),

[2111604002@mail2.gdut.edu.cn](mailto:2111604002@mail2.gdut.edu.cn) (L. Huang), [chunsing.lai@brunel.ac.uk](mailto:chunsing.lai@brunel.ac.uk) (C.S. Lai),

[jjayw@sustech.edu.cn](mailto:jjayw@sustech.edu.cn) (Y. Jia), [zhuoli.zhao@gdut.edu.cn](mailto:zhuoli.zhao@gdut.edu.cn) (Z. Zhao),

[lixuecong@gdut.edu.cn](mailto:lixuecong@gdut.edu.cn) (X. Li), [l.l.lai@ieee.org](mailto:l.l.lai@ieee.org) (L.L. Lai).

**Nomenclature**

**Constants and Sets:**

<b>P</b>	Nodal active power injection vector.
<b>Q</b>	Nodal reactive power injection vector.
<b>V</b>	Bus voltage magnitude vector.
<b>θ</b>	Bus voltage phase angle vector.
<b>G</b>	Bus conductance matrix.
<b>B, B'</b>	Bus susceptance matrices with or without considering shunt capacitor.
<b>M</b>	A matrix consisting of matrices <b>G, B, B'</b> .
<b>H, J, K, F</b>	Submatrices of the <b>M</b> inverse.
$S_{mn,i}^{Q-P}$	LAC-based shift factor of branch connecting bus $m$ to $n$ denotes the change of reactive power flow on branch connecting bus $m$ to $n$ , when one unit of active power is injected into bus $i$ .
$S_{mn,i}^{P-P}$	LAC-based shift factor of branch connecting bus $m$ to $n$ denotes the change of active power flow on branch connecting bus $m$ to $n$ , when one unit of active power is injected into bus $i$ .
$S_{m,i}^{V-P}$	LAC-based shift factor of bus $m$ denotes the change of voltage magnitude at bus $m$ , when one unit of active power is injected into bus $i$ .
$S_{mn,i}^{P-Q}$	LAC-based shift factor of branch connecting bus $m$ to $n$ denotes the change of active power flow on branch connecting bus $m$ to $n$ when one unit of reactive power is injected into bus $i$ .
$S_{mn,i}^{Q-Q}$	LAC-based shift factor of branch connecting bus $m$ to $n$ denotes the change of reactive power flow on branch connecting bus $m$ to $n$ , when one unit of reactive power is injected into bus $i$ .
$S_{m,i}^{V-Q}$	LAC-based shift factor of bus $m$ denotes the change of voltage magnitude at bus $m$ , when one unit of reactive power is injected into bus $i$ .
$T_{mn,i \rightarrow j}^{P-P}$	LAC-based power transfer distribution factor of branch connecting bus $m$ to $n$ denotes the change of active power flow on branch connecting bus $m$ to $n$ , when one unit of active power is transferred from bus $i$ to bus $j$ .
$T_{mn,i \rightarrow j}^{Q-P}$	LAC-based power transfer distribution factor of branch connecting bus $m$ to $n$ denotes the change of reactive power flow on branch connecting bus $m$ to $n$ , when one unit of active power is transferred from bus $i$ to bus $j$ .
$T_{m,i \rightarrow j}^{V-P}$	LAC-based power transfer distribution factor of bus $m$ denotes the change of voltage magnitude at bus $m$ , when one unit of active power is transferred from bus $i$ to bus $j$ .
$T_{mn,i \rightarrow j}^{P-Q}$	LAC-based power transfer distribution factor of branch connecting bus $m$ to $n$ denotes the change of active power flow on branch connecting bus $m$ to $n$ , when one unit of reactive power is transferred from bus $i$ to bus $j$ .

$T_{mn,i \rightarrow j}^{Q-Q}$	LAC-based power transfer distribution factor of branch connecting bus $m$ to $n$ denotes the change of reactive power flow on branch connecting bus $m$ to $n$ , when one unit of reactive power is transferred from bus $i$ to bus $j$ .
$T_{m,i \rightarrow j}^{V-Q}$	LAC-based power transfer distribution factor of bus $m$ denotes the change of voltage magnitude at bus $m$ , when one unit of reactive power is transferred from bus $i$ to bus $j$ .
$L_{mn,ij}^{P-P}$	LAC-based line outage distribution factor of branch connecting bus $m$ to $n$ denotes the change of active power flow on this branch caused by the outage of branch connecting bus $i$ to $j$ with pre-contingency active power flow of one unit.
$L_{mn,ij}^{Q-P}$	LAC-based line outage distribution factor of branch connecting bus $m$ to $n$ denotes the change of reactive power flow on this branch caused by the outage of branch connecting bus $i$ to $j$ with pre-contingency active power flow of one unit.
$L_{m,ij}^{V-P}$	LAC-based line outage distribution factor of bus $m$ denotes the change of voltage magnitude at bus $m$ caused by the outage of branch connecting bus $i$ to $j$ with pre-contingency active power flow of one unit.
$L_{mn,ij}^{P-Q}$	LAC-based line outage distribution factor of branch connecting bus $m$ to $n$ denotes the change of active power flow on this branch caused by the outage of branch connecting bus $i$ to $j$ with pre-contingency reactive power flow of one unit.
$L_{mn,ij}^{Q-Q}$	LAC-based line outage distribution factor of branch connecting bus $m$ to $n$ denotes the change of reactive power flow on this branch caused by the outage of branch connecting bus $i$ to $j$ with pre-contingency active power flow of one unit.
$L_{m,ij}^{V-Q}$	LAC-based line outage distribution factor of bus $m$ denotes the change of voltage magnitude at bus $m$ caused by the outage of branch connecting bus $i$ to $j$ with pre-contingency active power flow of one unit.
$\alpha, \beta$	Coefficients used to derive the LAC-based LODF.
$C_1, C_2, C_3$	Coefficients of different objective terms.
$V_{base}$	Voltage magnitude base.
$V_m^{min}, V_m^{max}$	Minimum/maximum voltage magnitude of bus $m$ .
$S_{mn}^{max}$	Maximum apparent power flow of branch connecting bus $m$ to $n$
$S_{mn}^{max,c}$	Maximum apparent power flow of branch connecting bus $m$ to $n$ in contingency states.

$P_g^{G,\min}, P_g^{G,\max}$	Minimum/maximum active power output of generator $g$ .
$Q_g^{G,\min}, Q_g^{G,\max}$	Minimum/maximum reactive power output of generator $g$ .
$P_d^D, Q_d^D$	Active and reactive load demand of load $d$ .
$S_L$	Set of branches.
$S_{AL}$	Set of branches forecasted to be affected by an extreme weather event.
$S_B$	Set of buses.
$S_G$	Set of generators.
$S_D$	Set of loads.
$S_{G,i}$	Set of generators connected to bus $i$ .
$S_{D,i}$	Set of loads connected to bus $i$ .
$NB$	Number of buses.
$NL$	Number of lines.
$i, m, n$	Indices for buses.
$g$	Index for generators.
$d$	Index for loads.
<b>Variables:</b>	
$P_g^G, Q_g^G$	Active and reactive power output of generator $g$ .
$P_i, Q_i$	Injected active and reactive power of bus $i$ .
$P_d^{ls}$	Active power load shedding in load $d$ .
$Q_d^{ls}$	Reactive power load shedding in load $d$ .
$R_{mn}$	Loading rate of active power on branch connecting bus $m$ to $n$ .
$P_{mn}^L, Q_{mn}^L$	Active/reactive power flow on branch connecting bus $m$ to $n$ .
$P_{mn}^{L,N-k}, Q_{mn}^{L,N-k}$	Post-contingency active and reactive power flow on branch connecting bus $m$ to $n$ of N-k contingency.
$V_m^{N-k}$	Voltage magnitude of bus $m$ after N-k contingency.
$s_{mn}^+, s_{mn}^-, t_{mn}^+, t_{mn}^-$	Auxiliary variables to linearize the objective term related to active power flow on branch connecting bus $m$ to $n$ .

power flow transfer after the initial failures. The DC power flow model was applied to construct transmission network security constraints in most of the above studies due to its excellent computational efficiency. However, since reactive power and voltage magnitude are not modeled in the DC model, the resulting solution cannot ensure that the voltage magnitude is within the allowable range, which may result in under-voltage and load shedding followed by a blackout, especially in extreme conditions. This paper presents an in-depth study of a linearized AC power flow (LAC) model with reactive power and voltage magnitude to derive sensitivity factors, including shift factors (LAC-SF) and line outage distribution factors (LAC-LODF), for pre-contingency and post-contingency power flow calculations for N-k contingencies. The authors then propose a resilience-constrained economic dispatch (LAC-RCED) strategy which takes into account the security constraints of the apparent power flow on the transmission line and the bus voltage magnitude under normal and contingency states, as well as optimization objectives to improve the power flow distribution in the transmission system.

Sensitivity factors reflect how the power flow variables (including power flows, voltage magnitudes, and phase angles)

change with the change of another variable (injected powers and power flows). Sensitivity factors of the DC power flow model have been extensively discussed and used in the literature. In [11,12], DC-based SF, power transfer distribution factor (PTDF), and LODF are defined and calculated in detail. In [13], an algorithm to construct an equivalent reduced power system model was proposed by approximating the PTDF and SF of the original system. In [14], the generation shift factors and LODF were used to distinguish between failure caused by power transfers due to the outage of other branches and actual faults of relays. However, these applications are limited to the DC model and can only reflect the characteristics of active power. LODF in the full AC power flow model was studied in [15–18]. However, if a sensitivity factor is calculated using the non-linear power flow equation, it depends not only on the topology of the system but also on the operation point of the system state, i.e., the power flow solution. Sensitivity factors of the AC power flow model are usually used for security analysis and do not apply to power system operation optimization problems. There is a lack of literature focus on the sensitivity analysis equations for linearized AC power flow models with reactive power and voltage magnitude, which is only dependent on the topology of the system and can be used in generation dispatch optimization problems. This paper aims to fill this knowledge gap.

Different LAC models with reactive power and voltage magnitude have been proposed in [19–21]. These linearized models are widely used in problems such as optimal power flow [22,23], available transfer capability [24], locational marginal price [25], transactions in distribution networks [26], due to their computational efficiency and accuracy. This paper refers to the LAC model proposed in [21] and presents in-depth studies about its application. Three kinds of linear sensitivity factors of this LAC model are proposed, namely, LAC-SF, LAC-PTDF, and LAC-LODF.

Based on the derived sensitivity factors, a LAC-based resilience-constrained economic dispatch model is proposed. Security constraints of N-k contingencies are necessary for a resilient generation dispatch scheme. However, it is hard to directly include the security constraints of all N-k contingency scenarios in an optimization problem of power system operation, since there are thousands of components in a grid. Bender decomposition is one of the widely used methods to solve large-scale security-constrained unit commitment or economic dispatch problems [27–30]. However, not all contingency constraints have an impact on the feasible region of these problems. Therefore, the computational efficiency could be improved by identifying active constraints and then incorporating only these constraints into the problem. Authors of [31] proposed an iterative LODF-based algorithm to find the active constraints that are binding the SCUC to consider the security constraints for N-1 contingency cases. The same idea was applied to the resilience-constrained economic dispatch model in [10] and a contingency constrained transmission expansion planning problem in [32]. However, all these three works are based on the LODF of the DC model. In this paper, based on the derived LAC-LODF, a modified iterative contingency filtering process is proposed to consider active N-1 and N-2 contingency constraints in the proposed LAC-RCED.

In summary, existing power dispatch optimization problems for improving system resilience rarely consider the security constraints on voltage and reactive power, and the resulting solutions are not safe enough. LODF applicable to optimization problems with N-k contingency constraints considering reactive power and voltage distribution is also lacking. This paper aims to fill these knowledge gaps. Table 1 shows the function comparison between this paper and other related works.

The main contributions of this paper are summarized as follows:

**Table 1**  
Function comparison between this study and related works (Y = yes, N = no).

Reference	Comparison of resilience enhancement strategies			Comparison of the derivation of sensitivity factors		
	Operation constraints of reactive power and voltage	Objectives in addition to generation costs	Efficient solutions for contingency constraints	Based on power flow models with reactive power and voltage	If only dependent on system topology	LODF for N-k contingency
[4]	N	N	Y	N	N	N
[5]	N	N	Y	N	N	N
[6]	N	Y	Y	N	N	N
[7]	N	N	Y	N	N	N
[8]	N	N	Y	N	N	N
[9]	N	Y	N	N	Y	N
[10]	N	Y	Y	N	Y	Y
[11]	N	N	N	N	Y	Y
[12]	N	N	N	N	Y	Y
[13]	N	N	N	N	Y	N
[14]	N	N	N	N	Y	N
[15]	N	N	N	Y	N	N
[16]	N	N	N	Y	N	N
[17]	N	N	N	Y	N	N
[18]	N	N	N	Y	N	Y
<b>This study</b>	Y	Y	Y	Y	Y	Y

1. Sensitivity analysis equations for a linearized power flow model with reactive power and voltage magnitude are proposed. Sensitivity factors, including SFs and LODFs, are derived for pre-contingency and post-contingency power flow calculations of N-k contingency cases.

2. Based on the derived sensitivity factors, a resilience-constrained economic dispatch strategy is developed, which considers the security constraints of N-1 contingency for all lines and N-2 contingency for the affected lines, as well as optimization objectives to improve the power flow distribution in the transmission system.

3. A modified iterative contingency filtering process is proposed to consider active N-1 and N-2 contingency constraints in the proposed optimization model. The maximum number of contingency constraints allowed to be added to the optimization problem in each iteration is predefined to make the process more applicable to large-scale systems.

The remainder of this paper is organized as below. Section 2 provides the equations for calculating the sensitivity factors, LAC-SF, LAC-PTDF, and LAC-LODF of the LAC model. In Section 3, the derived LAC-SF and LAC-LODF are applied to the proposed LAC-RCED model and the iterative contingency filtering algorithm is presented. Section 4 shows the case studies that validate the performance of the proposed model and solution techniques. Section 5 gives the conclusion, summarizes the experimental results and suggests future work.

## 2. Derivation of sensitivity factors of a LAC model

### 2.1. LAC model

The well-known AC power flow model for a power system is as follows:

$$P_i = \sum_{j \in S_B} G_{ij} V_i V_j \cos \theta_{ij} + \sum_{j \in S_B} B_{ij} V_i V_j \sin \theta_{ij} \quad (1)$$

$$Q_i = - \sum_{j \in S_B} B_{ij} V_i V_j \cos \theta_{ij} + \sum_{j \in S_B} G_{ij} V_i V_j \sin \theta_{ij}$$

$$P_{ij}^L = g_{ij} V_i (V_i - V_j \cos \theta_{ij}) - b_{ij} V_i V_j \sin \theta_{ij} \quad (2)$$

$$Q_{ij}^L = -V_i^2 \frac{b_{sh,ij}}{2} - b_{ij} V_i (V_i - V_j \cos \theta_{ij}) - g_{ij} V_i V_j \sin \theta_{ij}$$

According to the assumptions made in [21], these equations are approximately linearized as the following linear equations

with decoupled voltage magnitudes and phase angles.

$$P_i = - \sum_{j \in S_B} B'_{ij} \theta_j + \sum_{j \in S_B} G_{ij} V_j \quad (3)$$

$$Q_i = - \sum_{j \in S_B} G_{ij} \theta_j - \sum_{j \in S_B} B_{ij} V_j$$

$$P_{ij}^L = g_{ij} (V_i - V_j) - b_{ij} (\theta_i - \theta_j) \quad (4)$$

$$Q_{ij}^L = -b_{ij} (V_i - V_j) - g_{ij} (\theta_i - \theta_j)$$

The matrix form of (3) for a power system with multiple buses is as follows:

$$\begin{bmatrix} \mathbf{P} \\ \mathbf{Q} \end{bmatrix} = \begin{bmatrix} -\mathbf{B}' & \mathbf{G} \\ -\mathbf{G} & -\mathbf{B} \end{bmatrix} \begin{bmatrix} \boldsymbol{\theta} \\ \mathbf{V} \end{bmatrix} \quad (5)$$

Since the above equation is linear, the following equations can be easily obtained:

$$\begin{bmatrix} \Delta \mathbf{P} \\ \Delta \mathbf{Q} \end{bmatrix} = \begin{bmatrix} -\mathbf{B}' & \mathbf{G} \\ -\mathbf{G} & -\mathbf{B} \end{bmatrix} \begin{bmatrix} \Delta \boldsymbol{\theta} \\ \Delta \mathbf{V} \end{bmatrix} = \mathbf{M} \begin{bmatrix} \Delta \boldsymbol{\theta} \\ \Delta \mathbf{V} \end{bmatrix} \quad (6)$$

In this paper, a sensitivity analysis is performed for this LAC model to derive sensitivity factors for pre-contingency and post-contingency power flow calculations of N-k contingencies.

### 2.2. Derivation of the LAC-SF and LAC-PTDF

The derivation of LAC-SF and LAC-PTDF is shown in this section. LAC-SF for a branch and a bus is the sensitivity of power flows or bus voltage magnitude to the change in bus injections. It shows how the power flow on a branch or bus voltage magnitude will change if the injection at a bus is changed by one unit. LAC-PTDF reflects the change in the power flow on a branch and bus voltage magnitude when one unit of power is transferred from one bus of the network to another one.

To derive LAC-SF and LAC-PTDF,  $\Delta \boldsymbol{\theta}$  and  $\Delta \mathbf{V}$  needs to be calculated. However, since the matrix  $\mathbf{M}$  is singular, it cannot be directly inverted to calculate the unknown  $\Delta \boldsymbol{\theta}$  and  $\Delta \mathbf{V}$  via the known nodal active and reactive power injection  $\Delta \mathbf{P}$  and  $\Delta \mathbf{Q}$ . Based on the bus classification method widely used in power flow analysis, Eq. (6) needs to be reconstructed. According to the known and unknown variables of the slack bus, PV buses, and PQ buses, the following reduction could be performed.

1. Remove the row corresponding to the slack bus in  $\Delta \mathbf{P}$  and  $\Delta \boldsymbol{\theta}$ , and denote the reduced vector as  $\Delta \mathbf{P}^*$  and  $\Delta \boldsymbol{\theta}^*$ , respectively.

2. Remove the rows corresponding to the slack bus and PV buses in  $\Delta\mathbf{Q}$  and  $\Delta\mathbf{V}$ , and denote the reduced vector as  $\Delta\mathbf{Q}^*$  and  $\Delta\mathbf{V}^*$ .

3. Remove the row and column corresponding to the slack bus in  $-\mathbf{B}'$ , and denote the reduced matrix as  $-\mathbf{B}^*$ .

4. Remove the rows and columns corresponding to the slack bus and PV buses in  $-\mathbf{B}$ , and denote the reduced matrix as  $-\mathbf{B}^*$ .

5. Remove the row corresponding to the slack bus and columns corresponding to the slack bus and PV buses in  $\mathbf{G}$ , and denote the reduced matrix as  $\mathbf{G}_1^*$ .

6. Remove the column corresponding to the slack bus and rows corresponding to the slack buses and PV bus in  $\mathbf{G}$ , and denote the reduced matrix as  $-\mathbf{G}_{11}^*$ .

To express the relationship between the above original matrices and reduced matrices with mathematical expression. Two reduced identity matrices  $\mathbf{I}_1$  and  $\mathbf{I}_2$  are defined.  $\mathbf{I}_1$  is obtained by removing the row corresponding to the slack bus in an identity matrix with the size of  $NB \times NB$ .  $\mathbf{I}_2$  is obtained by removing the rows corresponding to slack bus and PV buses in an identity matrix with a size of  $NB \times NB$ . With  $\mathbf{I}_1$  and  $\mathbf{I}_2$ , the mathematical expressions of original matrices and reduced matrices are as follows:

$$\Delta\mathbf{P}^* = \mathbf{I}_1 \Delta\mathbf{P}, \quad \Delta\theta^* = \mathbf{I}_1 \Delta\theta \quad (7)$$

$$\begin{aligned} \Delta\mathbf{Q}^* &= \mathbf{I}_2 \Delta\mathbf{Q}, & \Delta\mathbf{V}^* &= \mathbf{I}_2 \Delta\mathbf{V} \\ -\mathbf{B}^* &= \mathbf{I}_1 (-\mathbf{B}') \mathbf{I}_1^T, & \mathbf{G}_1^* &= \mathbf{I}_1 \mathbf{G}_1 \mathbf{I}_1^T \\ -\mathbf{B}^* &= \mathbf{I}_2 (-\mathbf{B}) \mathbf{I}_2^T, & -\mathbf{G}_{11}^* &= \mathbf{I}_2 \mathbf{G}_1 \mathbf{I}_2^T \end{aligned} \quad (8)$$

Finally, the reduced LAC model for power flow analysis is reconstructed as follows:

$$\begin{bmatrix} \Delta\mathbf{P}^* \\ \Delta\mathbf{Q}^* \end{bmatrix} = \begin{bmatrix} -\mathbf{B}^* & \mathbf{G}_1^* \\ -\mathbf{G}_{11}^* & -\mathbf{B}^* \end{bmatrix} \begin{bmatrix} \Delta\theta^* \\ \Delta\mathbf{V}^* \end{bmatrix} = \mathbf{M}^* \begin{bmatrix} \Delta\theta^* \\ \Delta\mathbf{V}^* \end{bmatrix} \quad (9)$$

Note that matrix  $\mathbf{M}^*$  is no longer a singular matrix in (9). It is easy to calculate  $\Delta\theta^*$  and  $\Delta\mathbf{V}^*$  by inverting  $\mathbf{M}^*$  as bellow.

$$\begin{bmatrix} \Delta\theta^* \\ \Delta\mathbf{V}^* \end{bmatrix} = [\mathbf{M}^*]^{-1} \begin{bmatrix} \Delta\mathbf{P}^* \\ \Delta\mathbf{Q}^* \end{bmatrix} = \begin{bmatrix} \mathbf{H} & \mathbf{J} \\ \mathbf{K} & \mathbf{F} \end{bmatrix} \begin{bmatrix} \Delta\mathbf{P}^* \\ \Delta\mathbf{Q}^* \end{bmatrix} \quad (10)$$

With (4) and (10), the calculation of LAC-SF is conducted in this LAC model. In order to calculate  $S_{mn,i}^{P-P}$ , set the element in  $\Delta\mathbf{P}$  corresponding to bus  $i$  as 1, and the rest elements are set as 0, and denote this known vector as  $\Delta\mathbf{P}_i$ . At the same time, all elements of  $\Delta\mathbf{Q}$  are set to zero. Therefore, the expression of  $S_{mn,i}^{P-P}$  is as follows:

$$\begin{aligned} S_{mn,i}^{P-P} &= g_{mn} \Phi_{mn} \Delta\mathbf{V} - b_{mn} \Phi_{mn} \Delta\theta \\ &= g_{mn} \Phi_{mn} \mathbf{I}_2^T \mathbf{K} \mathbf{I}_1 \Delta\mathbf{P}_i - b_{mn} \Phi_{mn} \mathbf{I}_1^T \mathbf{H} \mathbf{I}_1 \Delta\mathbf{P}_i \end{aligned} \quad (11)$$

where  $\Phi_{mn} = [0, \dots, 1, \dots, -1, \dots, 0]$ ,  $\Phi_{mn}(m) = 1$ ,  $\Phi_{mn}(n) = -1$ .

Shift factor  $S_{mn,i}^{Q-P}$  for branch  $mn$  denotes the change of reactive power flow on branch  $mn$ , when one unit of active power is injected into bus  $i$ . The expression of LAC-SF  $S_{mn,i}^{Q-P}$  is as follows:

$$\begin{aligned} S_{mn,i}^{Q-P} &= -b_{mn} \Phi_{mn} \Delta\mathbf{V} - g_{mn} \Phi_{mn} \Delta\theta \\ &= -b_{mn} \Phi_{mn} \mathbf{I}_2^T \mathbf{K} \mathbf{I}_1 \Delta\mathbf{P}_i - g_{mn} \Phi_{mn} \mathbf{I}_1^T \mathbf{H} \mathbf{I}_1 \Delta\mathbf{P}_i \end{aligned} \quad (12)$$

Shift factor  $S_{m,i}^{V-P}$  for bus  $m$  denotes the change of voltage magnitude at bus  $m$  when one unit of active power is injected into bus  $i$ . The expression of shift factor  $S_{m,i}^{V-P}$  is as follows:

$$S_{m,i}^{V-P} = \kappa \mathbf{I}_2^T \mathbf{K} \mathbf{I}_1 \Delta\mathbf{P}_i \quad (13)$$

where  $\kappa = [0, \dots, 1, \dots, 0]$ ,  $\kappa(m) = 1$ .

Similarly, the expressions of LAC-SF related to reactive power injection are as follows:

$$\begin{aligned} S_{mn,i}^{P-Q} &= g_{mn} \Phi_{mn} \mathbf{I}_2^T \mathbf{F} \mathbf{I}_2 \Delta\mathbf{Q}_i - b_{mn} \Phi_{mn} \mathbf{I}_1^T \mathbf{J} \mathbf{I}_2 \Delta\mathbf{Q}_i \\ S_{mn,i}^{Q-Q} &= -b_{mn} \Phi_{mn} \mathbf{I}_2^T \mathbf{F} \mathbf{I}_2 \Delta\mathbf{Q}_i - g_{mn} \Phi_{mn} \mathbf{I}_1^T \mathbf{J} \mathbf{I}_2 \Delta\mathbf{Q}_i \\ S_{m,i}^{V-Q} &= \kappa \mathbf{I}_2^T \mathbf{F} \mathbf{I}_2 \Delta\mathbf{Q}_i \end{aligned} \quad (14)$$

where  $\Delta\mathbf{Q}_i = [0, \dots, 1, \dots, 0]^T$ ,  $\Delta\mathbf{Q}_i(i) = 1$ .

After deriving LAC-SF, LAC-PTDF can be calculated directly by using LAC-SF according to the equivalent networks shown in Fig. 1. As shown in Fig. 1(b) and (c),  $\Delta P_{mn,i}^L + j\Delta Q_{mn,i}^L$  and  $\Delta P_{mn,j}^L + j\Delta Q_{mn,j}^L$  are power flow on branch  $mn$  determined by the injection of  $\Delta P_i + j\Delta Q_i$  at bus  $i$  and the injection of  $\Delta P_j + j\Delta Q_j$  at bus  $j$ , respectively.  $\Delta V_{m,i}$  and  $\Delta V_{m,j}$  are bus voltage magnitudes. With LAC-SF, the expressions of  $\Delta P_{mn,i}^L$ ,  $\Delta Q_{mn,i}^L$ ,  $\Delta P_{mn,j}^L$ ,  $\Delta Q_j$ ,  $\Delta V_{m,i}$  and  $\Delta V_{m,j}$  are as follows:

$$\begin{aligned} \Delta P_{mn,i}^L &= S_{mn,i}^{P-P} \Delta P_i + S_{mn,i}^{P-Q} \Delta Q_i \\ \Delta Q_{mn,i}^L &= S_{mn,i}^{Q-P} \Delta P_i + S_{mn,i}^{Q-Q} \Delta Q_i \end{aligned} \quad (15)$$

$$\begin{aligned} \Delta P_{mn,j}^L &= S_{mn,j}^{P-P} \Delta P_j + S_{mn,j}^{P-Q} \Delta Q_j \\ \Delta Q_{mn,j}^L &= S_{mn,j}^{Q-P} \Delta P_j + S_{mn,j}^{Q-Q} \Delta Q_j \end{aligned} \quad (16)$$

$$\Delta V_{m,i} = S_{m,i}^{V-P} \Delta P_i + S_{m,i}^{V-Q} \Delta Q_i \quad (17)$$

$$\Delta V_{m,j} = S_{m,j}^{V-P} \Delta P_j + S_{m,j}^{V-Q} \Delta Q_j \quad (18)$$

According to the relationship between power flows and the relationship between bus voltage magnitudes shown on the left and right sides of the equivalent networks, the following equations can be obtained:

$$\Delta P_{mn,i \rightarrow j}^L = \Delta P_{mn,i}^L - \Delta P_{mn,j}^L \quad (19)$$

$$\Delta Q_{mn,i \rightarrow j}^L = \Delta Q_{mn,i}^L - \Delta Q_{mn,j}^L \quad (20)$$

$$\Delta V_{m,i \rightarrow j} = \Delta V_{m,i} - \Delta V_{m,j} \quad (20)$$

By substituting (15) and (16) into (19), (17) and (18) into (20), the following equations can be obtained:

$$\Delta P_{mn,i \rightarrow j}^L = S_{mn,i}^{P-P} \Delta P_i - S_{mn,j}^{P-P} \Delta P_j + S_{mn,i}^{P-Q} \Delta Q_i - S_{mn,j}^{P-Q} \Delta Q_j \quad (21)$$

$$\Delta Q_{mn,i \rightarrow j}^L = S_{mn,i}^{Q-P} \Delta P_i - S_{mn,j}^{Q-P} \Delta P_j + S_{mn,i}^{Q-Q} \Delta Q_i - S_{mn,j}^{Q-Q} \Delta Q_j \quad (22)$$

$$\Delta V_{m,i \rightarrow j} = S_{m,i}^{V-P} \Delta P_i - S_{m,j}^{V-P} \Delta P_j + S_{m,i}^{V-Q} \Delta Q_i - S_{m,j}^{V-Q} \Delta Q_j \quad (22)$$

According to the definition of LAC-PTDF, by substituting  $\Delta P_i = \Delta P_j = 1$ ,  $\Delta Q_i = \Delta Q_j = 1$  into (21) and (22), it is easy to obtain four kinds of LAC-PTDF for a branch and two for a bus regarding active and reactive power transfer, respectively. The expressions of the above six kinds of LAC-PTDF are as follows:

$$\begin{aligned} T_{mn,i \rightarrow j}^{P-P} &= S_{mn,i}^{P-P} - S_{mn,j}^{P-P} & T_{mn,i \rightarrow j}^{Q-Q} &= S_{mn,i}^{Q-Q} - S_{mn,j}^{Q-Q} \\ T_{mn,i \rightarrow j}^{P-Q} &= S_{mn,i}^{P-Q} - S_{mn,j}^{P-Q} & T_{m,i \rightarrow j}^{V-P} &= S_{m,i}^{V-P} - S_{m,j}^{V-P} \\ T_{mn,i \rightarrow j}^{Q-P} &= S_{mn,i}^{Q-P} - S_{mn,j}^{Q-P} & T_{m,i \rightarrow j}^{V-Q} &= S_{m,i}^{V-Q} - S_{m,j}^{V-Q} \end{aligned} \quad (23)$$

The specific definition for each kind of the above LAC-PTDF is explained in the nomenclature table. So far, we have provided formulas for calculating LAC-SF and LAC-PTDF in the introduced LAC model. How LAC-LODF is calculated will be discussed in the next section.

### 2.3. Derivation of the LAC-LODF for N-1 contingency

LODF is widely employed to determine the effects of contingent line outages. In the DC power flow model, the LODF for a specified branch outage is the incremental active power flow on the monitored branches caused by the outage of a contingent branch with a pre-outage active power flow of one unit. In

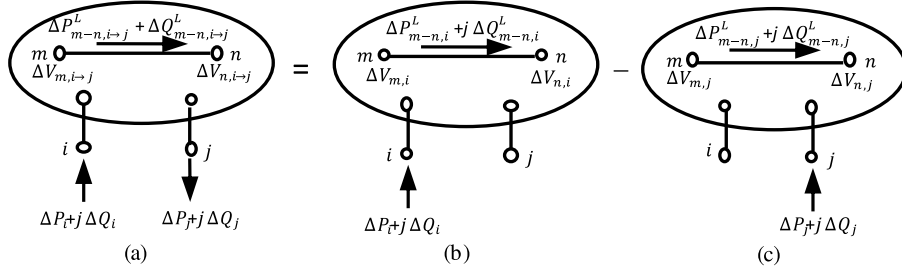


Fig. 1. Equivalent networks for the derivation of LAC-PTDF based on LAC-SF.

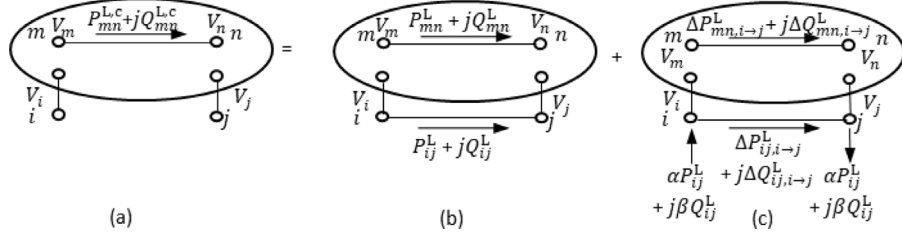


Fig. 2. Equivalent networks under the outage of branch  $ij$ .

this paper, LAC-LODF related to both active and reactive power flow is studied. Similar to LAC-SF and LAC-PTDF discussed above, six kinds of LAC-LODF including  $L^{P-P}$ ,  $L^{P-Q}$ ,  $L^{Q-P}$ ,  $L^{Q-Q}$ ,  $L^{V-P}$  and  $L^{V-Q}$  are presented in this work. With these LAC-LODF, the post-contingency power flow of a branch or post-contingency bus voltage magnitude of a bus can be calculated by the following equations:

$$P_{mn}^{L,N-1} = P_{mn}^L + L_{mn,ij}^{P-P} \cdot P_{ij}^L + L_{mn,ij}^{P-Q} \cdot Q_{ij}^L \quad (24)$$

$$Q_{m-n}^{L,N-1} = Q_{mn}^L + L_{mn,ij}^{Q-P} \cdot P_{ij}^L + L_{mn,ij}^{Q-Q} \cdot Q_{ij}^L \quad (25)$$

To derive the calculation approach of the above LAC-LODF, equivalent networks under the outage of branch  $ij$  are shown in Fig. 2. Fig. 2(a) and (b) show the system states after and before the failure respectively, including line power flow and node voltage. Fig. 2(c) is the transition state of system failure, including the variation change of power flow and voltage before and after the failure. The term  $\alpha P_{ij}^L + j\beta Q_{ij}^L$  is fictitious power injected at bus  $i$  and withdrawn at bus  $j$ . The terms  $\Delta P_{mn,i→j}^L + j\Delta Q_{mn,i→j}^L$  and  $\Delta P_{ij,i→j}^L + j\Delta Q_{ij,i→j}^L$  are incremental power flow on branch  $mn$  and  $ij$  due to the power transfer of  $\alpha P_{ij}^L + j\beta Q_{ij}^L$  from bus  $i$  to bus  $j$ . According to the nodal power balance at bus  $i$  or bus  $j$ , the following equations can be obtained:

$$P_{ij}^L + T_{ij,i→j}^{P-P} \cdot \alpha P_{ij}^L + T_{ij,i→j}^{P-Q} \cdot \beta Q_{ij}^L = \alpha P_{ij}^L \quad (26)$$

$$Q_{ij}^L + T_{ij,i→j}^{Q-P} \cdot \alpha P_{ij}^L + T_{ij,i→j}^{Q-Q} \cdot \beta Q_{ij}^L = \beta Q_{ij}^L \quad (27)$$

By solving (26) and (27) simultaneously, Eq. (28) can be obtained:

$$\alpha P_{ij}^L = \frac{(1 - T_{ij,i→j}^{Q-Q}) P_{ij}^L + T_{ij,i→j}^{P-Q} \cdot Q_{ij}^L}{(1 - T_{ij,i→j}^{P-P})(1 - T_{ij,i→j}^{Q-Q}) - T_{ij,i→j}^{P-Q} \cdot T_{ij,i→j}^{Q-P}} = a \cdot P_{ij}^L + b \cdot Q_{ij}^L$$

$$\beta Q_{ij}^L = \frac{(1 - T_{ij,i→j}^{Q-Q}) Q_{ij}^L + T_{ij,i→j}^{Q-P} \cdot P_{ij}^L}{(1 - T_{ij,i→j}^{P-P})(1 - T_{ij,i→j}^{Q-Q}) - T_{ij,i→j}^{P-Q} \cdot T_{ij,i→j}^{Q-P}} = c \cdot P_{ij}^L + d \cdot Q_{ij}^L \quad (28)$$

According to the relationship between power flows and the relationship between bus voltage magnitudes shown on the left and

right sides of the equivalent networks, the following equations can be obtained:

$$P_{mn}^{L,N-1} = P_{mn}^L + \Delta P_{mn,i→j}^L = P_{mn}^L + T_{mn,i→j}^{P-P} \cdot \alpha P_{ij}^L + T_{mn,i→j}^{P-Q} \cdot \beta Q_{ij}^L$$

$$= P_{mn}^L + (T_{mn,i→j}^{P-P} \cdot a + T_{mn,i→j}^{P-Q} \cdot c) \cdot P_{ij}^L + (T_{mn,i→j}^{P-P} \cdot b + T_{mn,i→j}^{P-Q} \cdot d) \cdot Q_{ij}^L \quad (29)$$

$$Q_{m-n}^{L,N-1} = Q_{mn}^L + \Delta Q_{mn,i→j}^L = Q_{mn}^L + T_{mn,i→j}^{Q-P} \cdot \alpha P_{ij}^L + T_{mn,i→j}^{Q-Q} \cdot \beta Q_{ij}^L$$

$$= Q_{mn}^L + (T_{mn,i→j}^{Q-P} \cdot a + T_{mn,i→j}^{Q-Q} \cdot c) \cdot P_{ij}^L + (T_{mn,i→j}^{Q-P} \cdot b + T_{mn,i→j}^{Q-Q} \cdot d) \cdot Q_{ij}^L \quad (30)$$

$$V_m^{N-1} = V_m + \Delta V_{m,i→j} = V_m + T_{m,i→j}^{V-P} \alpha P_{ij}^L + T_{m,i→j}^{V-Q} \beta Q_{ij}^L$$

$$= V_m + (T_{m,i→j}^{V-P} \cdot a + T_{m,i→j}^{V-Q} \cdot c) \cdot P_{ij}^L + (T_{m,i→j}^{V-P} \cdot b + T_{m,i→j}^{V-Q} \cdot d) \cdot Q_{ij}^L \quad (31)$$

By comparing (29), (30) and (31) with (24) and (25), we have the following expressions of different kinds of LAC-LODF:

$$L_{mn,ij}^{P-P} = T_{mn,i→j}^{P-P} \cdot a + T_{mn,i→j}^{P-Q} \cdot c \quad L_{mn,ij}^{P-Q} = T_{mn,i→j}^{P-P} \cdot b + T_{mn,i→j}^{P-Q} \cdot d$$

$$L_{mn,ij}^{Q-P} = T_{mn,i→j}^{Q-P} \cdot a + T_{mn,i→j}^{Q-Q} \cdot c \quad L_{mn,ij}^{Q-Q} = T_{mn,i→j}^{Q-P} \cdot b + T_{mn,i→j}^{Q-Q} \cdot d$$

$$L_{m,ij}^{V-P} = T_{m,i→j}^{V-P} \cdot a + T_{m,i→j}^{V-Q} \cdot c \quad L_{m,ij}^{V-Q} = T_{m,i→j}^{V-P} \cdot b + T_{m,i→j}^{V-Q} \cdot d \quad (32)$$

So far, the derivation of LAC-SF, LAC-PTDF, and LAC-LODF for N-1 contingency is completed. The LAC-LODF for N-k contingency will be presented in the next section.

#### 2.4. Derivation of the LAC-LODF for N-k contingencies

This section extends the LAC-LODF derived in the previous section based on N-1 contingency to the LAC-LODF applicable to N-k contingencies. Suppose that there are  $k$  line failures in an N-k contingency case, which are named as  $L1$  to  $Lk$  and included in the set  $Lf = [L1, \dots, Lk]$ . The post-contingency power flow solution of branch  $mn$  and bus  $m$  can be calculated by using the LAC-LODF

for the N-k contingency case by using the following equation:

$$\begin{aligned}
 P_{mn}^{L,N-k} &= P_{mn}^L + L_{mn,lf,L1}^{P-P} \cdot P_{L1}^L + L_{mn,lf,L1}^{P-Q} \cdot Q_{L1}^L + \dots \\
 &\quad + L_{mn,lf,Lk}^{P-P} \cdot P_{Lk}^L + L_{mn,lf,Lk}^{P-Q} \cdot Q_{Lk}^L \\
 Q_{mn}^{L,N-k} &= Q_{mn}^L + L_{mn,lf,L1}^{Q-P} \cdot P_{L1}^L + L_{mn,lf,L1}^{Q-Q} \cdot Q_{L1}^L + \dots \\
 &\quad + L_{mn,lf,Lk}^{Q-P} \cdot P_{Lk}^L + L_{mn,lf,Lk}^{Q-Q} \cdot Q_{Lk}^L \\
 V_m^{N-k} &= V_m + L_{m,lf,L1}^{V-P} \cdot P_{L1}^L + L_{m,lf,L1}^{V-Q} \cdot Q_{L1}^L + \dots \\
 &\quad + L_{m,lf,Lk}^{V-P} \cdot P_{Lk}^L + L_{m,lf,Lk}^{V-Q} \cdot Q_{Lk}^L
 \end{aligned} \tag{33}$$

Similar to the derivation of the LAC-LODF for N-1 contingency cases, the LAC-LODF for N-k contingency cases is derived by injecting and withdrawing virtual power at the two ends of the failure lines. The relationship between the pre-contingency power flow and the virtual power is as follows:

$$\begin{aligned}
 \begin{bmatrix} P_{L1}^L \\ Q_{L1}^L \\ \vdots \\ P_{Lk}^L \\ Q_{Lk}^L \end{bmatrix} &= \begin{bmatrix} 1 - T_{L1,L1}^{P-P} & -T_{L1,L1}^{P-Q} & \dots & -T_{L1,Lk}^{P-P} & -T_{L1,Lk}^{P-Q} \\ -T_{L1,L1}^{Q-P} & 1 - T_{L1,L1}^{Q-Q} & \dots & -T_{L1,Lk}^{Q-P} & -T_{L1,Lk}^{Q-Q} \\ \vdots & \vdots & \vdots & \vdots & \vdots \\ -T_{Lk,L1}^{P-P} & -T_{Lk,L1}^{P-Q} & \dots & 1 - T_{Lk,Lk}^{P-P} & -T_{Lk,Lk}^{P-Q} \\ -T_{Lk,L1}^{Q-P} & -T_{Lk,L1}^{Q-Q} & \dots & -T_{Lk,Lk}^{Q-P} & 1 - T_{Lk,Lk}^{Q-Q} \end{bmatrix} \\
 &\quad \cdot \begin{bmatrix} \alpha_1 P_{L1}^L \\ \beta_1 Q_{L1}^L \\ \vdots \\ \alpha_k P_{Lk}^L \\ \beta_k Q_{Lk}^L \end{bmatrix}
 \end{aligned} \tag{34}$$

By reformulating (34), we have the following equation:

$$\begin{aligned}
 \begin{bmatrix} \alpha_1 P_{L1}^L \\ \beta_1 Q_{L1}^L \\ \vdots \\ \alpha_k P_{Lk}^L \\ \beta_k Q_{Lk}^L \end{bmatrix} &= \begin{bmatrix} 1 - T_{L1,L1}^{P-P} & -T_{L1,L1}^{P-Q} & \dots & -T_{L1,Lk}^{P-P} & -T_{L1,Lk}^{P-Q} \\ -T_{L1,L1}^{Q-P} & 1 - T_{L1,L1}^{Q-Q} & \dots & -T_{L1,Lk}^{Q-P} & -T_{L1,Lk}^{Q-Q} \\ \vdots & \vdots & \vdots & \vdots & \vdots \\ -T_{Lk,L1}^{P-P} & -T_{Lk,L1}^{P-Q} & \dots & 1 - T_{Lk,Lk}^{P-P} & -T_{Lk,Lk}^{P-Q} \\ -T_{Lk,L1}^{Q-P} & -T_{Lk,L1}^{Q-Q} & \dots & -T_{Lk,Lk}^{Q-P} & 1 - T_{Lk,Lk}^{Q-Q} \end{bmatrix}^{-1} \\
 &\quad \cdot \begin{bmatrix} P_{L1}^L \\ Q_{L1}^L \\ \vdots \\ P_{Lk}^L \\ Q_{Lk}^L \end{bmatrix} \triangleq \mathbf{W} \cdot \begin{bmatrix} P_{L1}^L \\ Q_{L1}^L \\ \vdots \\ P_{Lk}^L \\ Q_{Lk}^L \end{bmatrix}
 \end{aligned} \tag{35}$$

After getting the virtual injected power, the incremental active power flow on branch  $mn$  can be calculated using LAC-SF, as below:

$$\begin{aligned}
 P_{mn}^{L,N-k} - P_{mn}^L &= \Delta P_{mn}^L = \begin{bmatrix} T_{mn,L1}^{P-P} \\ T_{mn,L1}^{P-Q} \\ \vdots \\ T_{mn,Lk}^{P-P} \\ T_{mn,Lk}^{P-Q} \end{bmatrix}^T \cdot \begin{bmatrix} \alpha_1 P_{L1}^L \\ \beta_1 Q_{L1}^L \\ \vdots \\ \alpha_k P_{Lk}^L \\ \beta_k Q_{Lk}^L \end{bmatrix} \\
 &= \begin{bmatrix} T_{mn,L1}^{P-P} \\ T_{mn,L1}^{P-Q} \\ \vdots \\ T_{mn,Lk}^{P-P} \\ T_{mn,Lk}^{P-Q} \end{bmatrix}^T \cdot \mathbf{W} \cdot \begin{bmatrix} P_{L1}^L \\ Q_{L1}^L \\ \vdots \\ P_{Lk}^L \\ Q_{Lk}^L \end{bmatrix}
 \end{aligned} \tag{36}$$

Combining (33) and (36), the expression of the LAC-LODF applicable to post-contingency active power flow calculation in an N-k contingency case is as follows:

$$\begin{bmatrix} L_{mn,lf,L1}^{P-P} \\ L_{mn,lf,L1}^{P-Q} \\ \vdots \\ L_{mn,lf,Lk}^{P-P} \\ L_{mn,lf,Lk}^{P-Q} \end{bmatrix} = \begin{bmatrix} T_{mn,L1}^{P-P} \\ T_{mn,L1}^{P-Q} \\ \vdots \\ T_{mn,Lk}^{P-P} \\ T_{mn,Lk}^{P-Q} \end{bmatrix}^T \cdot \mathbf{W} \tag{37}$$

Similarly, the expressions of the LAC-LODF applicable to post-contingency reactive power flow and bus voltage magnitude calculation in an N-k contingency case are as follows:

$$\begin{aligned}
 \begin{bmatrix} L_{mn,lf,L1}^{Q-P} \\ L_{mn,lf,L1}^{Q-Q} \\ \vdots \\ L_{mn,lf,Lk}^{Q-P} \\ L_{mn,lf,Lk}^{Q-Q} \end{bmatrix} &= \begin{bmatrix} T_{mn,L1}^{Q-P} \\ T_{mn,L1}^{Q-Q} \\ \vdots \\ T_{mn,Lk}^{Q-P} \\ T_{mn,Lk}^{Q-Q} \end{bmatrix}^T \cdot \mathbf{W} \\
 \begin{bmatrix} L_{m,lf,L1}^{V-P} \\ L_{m,lf,L1}^{V-Q} \\ \vdots \\ L_{m,lf,Lk}^{V-P} \\ L_{m,lf,Lk}^{V-Q} \end{bmatrix} &= \begin{bmatrix} T_{m,L1}^{V-P} \\ T_{m,L1}^{V-Q} \\ \vdots \\ T_{m,Lk}^{V-P} \\ T_{m,Lk}^{V-Q} \end{bmatrix}^T \cdot \mathbf{W}
 \end{aligned} \tag{38}$$

So far, the derivation of LAC-SF, LAC-PTDF, and LAC-LODF for pre-contingency and post-contingency power flow calculation for an N-k contingency case is completed. The derived LAC-SF and LAC-LODF will be used in the proposed LAC-RCED to establish the security constraints to ensure the power flow and bus voltage magnitude within the operating limits in the next section.

### 3. LAC-based resilience-constrained economic dispatch model

This section presents the mathematical formulation of the LAC-RCED model, where the LAC power flow model discussed above is used for power flow calculations in the base case. An iterative contingency filtering process based on the LAC-LODF discussed above is given to screen out violated contingency scenarios and incorporate the corresponding security constraints into the LAC-RCED model to ensure that the power flow and bus voltage magnitude are within the operating limits.

#### 3.1. LAC-RCED without considering contingency constraints

In blackouts during extreme events, massive power flow transfer often occurs after the initial failures caused by the event. The initial failures develop into overloaded cascading failures that eventually lead to blackouts. If LAC-RCED can improve the power flow distribution in the network to prevent massive power flow transfer after disturbance or to increase the available transmission capacity of the transmission line, the probability of blackouts caused by cascading failures could be reduced. The operational resilience of the power system could be enhanced. Referring to [10], the objective function of LAC-RCED is to minimize the generation cost as well as improve the power flow distribution in the transmission system. Two objective terms related to active power flow on transmission lines are considered to realize the goal. The first term aims to reduce the power flow in specific branches forecasted to be affected by an extreme weather event, which has a high probability of failure. Reducing the power flow

of these branches can avoid large-scale power transfer once there is a contingency caused by an extreme weather event. The second term aims to make the power flow relatively uniform to avoid overloaded or lightly loaded branches in the whole network. The mathematical expression of the objective function of the proposed LAC-RCED model is as follows:

$$\begin{aligned} \text{Min} \quad & \sum_{g \in S_G} f_g(P_g^G) + C_1 \cdot \sum_{mn \in S_{AL}} R_{mn} + C_2 \cdot \sum_{mn \in S_L} \left| R_{mn} - \frac{1}{NL} \sum_{mn \in S_L} R_{mn} \right| \\ & + C_3 \cdot \sum_{d \in S_D} (P_d^{ls} + Q_d^{ls}) \end{aligned} \quad (40)$$

where  $\sum_{g \in S_G} f_g(P_g^G)$  is the generation cost of all generators;  $f_g(P_g^G) = a_g(P_g^G)^2 + b_g P_g^G + c_g$ ;  $\sum_{mn \in S_{AL}} R_{mn}$  is the first penalty term, where  $R_{mn} = \left| \frac{P_{mn}^L}{S_{mn}^{\max}} \right|$  is the loading rate of the line  $mn$ ;  $\sum_{mn \in S_L} \left| R_{mn} - \frac{1}{NL} \sum_{mn \in S_L} R_{mn} \right|$  is the second penalty term;  $\sum_{d \in S_D} (P_d^{ls} + Q_d^{ls})$  is total unserved active power and reactive power of the system, where  $P_d^{ls}$  and  $Q_d^{ls}$  are unserved active power and reactive power of load  $d$  respectively, and the modeling method is from [33,34]; the system itself may not be satisfied with the N-k security criterion, therefore, the unserved active power and reactive power variables are needed to ensure the feasibility of the optimization problem.  $C_1$  is the coefficient of the first penalty term and  $C_2$  is the coefficient of the second penalty term.  $C_1$  and  $C_2$  are determined by comparing the values of the two penalty terms and the generation cost directly;  $C_3$  is the coefficient of penalty term for load unserved;  $C_3$  is a large value to avoid load unserved in the normal operation. The system itself may not satisfy the N-k security criterion, therefore, the unserved active power and reactive power variables are needed to ensure the feasibility of the optimization problem.

In (40), the first penalty term penalizes the loading rate of the line in the affected area. Because these lines are more preferably likely to fail due to the effect of the extreme event, we aim to reduce the power flow of these affected lines appropriately. On one hand, it reduces the probability of overload failures on these lines, and on the other hand, prevents large-scale power flow transfer when they are damaged by extreme events. The second penalty term penalizes the uniformity of the flow distribution of all lines, aiming to avoid some lines undertaking heavy loads and easy to suffer overload outages when there is a disturbance. The above two absolute value terms make the problem hard to be solved in the optimization problem. According to the method of optimization with absolute values, the above objective term can be linearized by introducing some auxiliary variables and constraints. The linearized form of the above objective function is as follows:

$$\begin{aligned} \text{Min} \quad & \sum_{g \in S_G} f_g(P_g^G) + C_1 \cdot \sum_{mn \in S_{AL}} R_{mn} + C_2 \cdot \sum_{mn \in S_L} (t_{mn}^+ + t_{mn}^-) \\ & + C_3 \cdot \sum_{d \in S_D} (P_d^{ls} + Q_d^{ls}) \\ \text{s.t.} \quad & R_{mn} = s_{mn}^+ + s_{mn}^- \quad \forall mn \in S_L \\ & \frac{P_{mn}^L}{S_{mn}^{\max}} - s_{mn}^+ + s_{mn}^- = 0 \quad \forall mn \in S_L \\ & 0 \leq s_{mn}^+ \leq M \cdot \mu_{mn} \quad 0 \leq s_{mn}^- \leq M \cdot (1 - \mu_{mn}) \\ & \mu_{mn} \in \{0, 1\} \quad \forall mn \in S_L \\ & R_{mn} - \frac{\sum_{mn \in S_L} R_{mn}}{NL} - t_{mn}^+ + t_{mn}^- = 0 \quad \forall mn \in S_L \\ & t_{mn}^+ \geq 0, t_{mn}^- \geq 0 \quad \forall mn \in S_L \end{aligned} \quad (41)$$

The operational constraints of the LAC-RCED model are the same as those of the traditional AC optimal power flow model. The differences are the ways the power flow and bus voltage magnitude are calculated.

$$P_i = \sum_{g \in S_{G,i}} P_g^G + \sum_{d \in S_{D,i}} (P_d^D - P_d^{ls}) \quad \forall i \in S_B \quad (42)$$

$$\begin{aligned} Q_i &= \sum_{g \in S_{G,i}} Q_g^G + \sum_{d \in S_{D,i}} (Q_d^D - Q_d^{ls}) \quad \forall i \in S_B \\ P_i &= - \sum_{j \in S_B} B'_{ij} \theta_j + \sum_{j \in S_B} G_{ij} V_j \quad \forall i \in S_B \\ Q_i &= - \sum_{j \in S_B} G_{ij} \theta_j - \sum_{j \in S_B} B_{ij} V_j \quad \forall i \in S_B \end{aligned} \quad (43)$$

$$\begin{aligned} P_{mn}^L &= g_{mn} (V_m - V_n) - b_{mn} (\theta_m - \theta_n) \quad \forall mn \in S_L \\ Q_{mn}^L &= -b_{mn} (V_m - V_n) - g_{mn} (\theta_m - \theta_n) \quad \forall mn \in S_L \\ P_g^{G,\min} &\leq P_g^G \leq P_g^{G,\max} \quad \forall g \in S_G \\ Q_g^{G,\min} &\leq Q_g^G \leq Q_g^{G,\max} \quad \forall g \in S_G \end{aligned} \quad (44)$$

$$\begin{aligned} 0 &\leq P_d^{ls} \leq P_d^D \quad \forall d \in S_D \\ 0 &\leq Q_d^{ls} \leq Q_d^D \quad \forall d \in S_D \end{aligned} \quad (45)$$

$$(P_{mn}^L)^2 + (Q_{mn}^L)^2 \leq (S_{mn}^{\max})^2 \quad \forall mn \in S_{AL} \quad (46)$$

$$V_m^{\min} \leq V_m \leq V_m^{\max} \quad \forall m \in S_B \quad (47)$$

Eq. (42) represents the active and reactive power injections at buses. Eq. (43) represents power flows on branches and voltage magnitudes at buses, which are calculated by LAC-SF. Constraints in (44) are the limits of the active and reactive power output of generators. Constraints in (45) limit the range of load shedding. Constraints in (46) are the apparent power flow limit. Constraints in (47) are the voltage magnitude limit. After solving LAC-RCED without contingency constraints, a resilient generation dispatch solution can be obtained, in which both power flow and bus voltage magnitude are within their operating limits in the base case.

### 3.2. Iterative contingency filtering process for LAC-RCED with contingency constraints

To enhance system resilience against transmission line N-k outage caused by extreme events, N-1 contingency constraints of all branches and N-2 contingency constraints for lines affected by an extreme weather event are considered in the proposed LAC-RCED. To reduce computational complexity, security constraints for all contingency cases are not directly modeled in the optimization model. In this work, an iterative contingency filtering algorithm based on the derived LAC-LODF is given to screen out violated contingency cases and incorporate the corresponding security constraints into the LAC-RCED.

In addition, since  $\mu_{mn}$  is a binary variable that makes the LAC-RCED model difficult to be solved, the LAC-based economic dispatch (LAC-ED) without penalty terms is first solved to determine the value of  $\mu_{mn}$ . The mathematical expression of the LAC-ED model without contingency constraints is as follows:

$$\text{Min} \quad \sum_{g \in S_G} f_g(P_g^G) + C_3 \cdot \sum_{d \in S_D} (P_d^{ls} + Q_d^{ls}) \quad (48)$$

s.t. (42)–(47).

The flowchart of the iterative contingency filtering algorithm for LAC-RCED with contingency constraints is shown in Fig. 3.

The solution procedure is as follows:

Step 1: Solve the LAC-ED problem without contingency constraints and obtain the flow direction of each branch. Set  $\mu_{mn}$

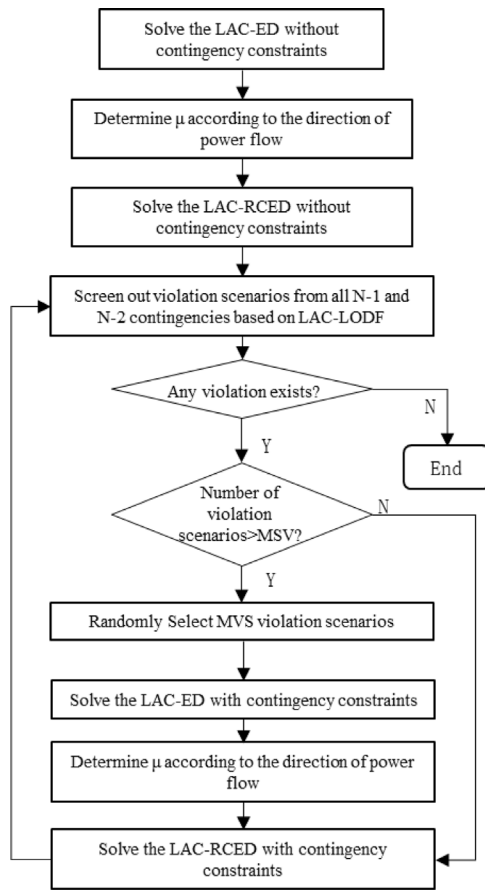


Fig. 3. Flowchart of the iterative contingency filtering algorithm.

in the LAC-RCED according to the obtained direction of power flow. When the power flow of branch  $mn$  is positive, set  $\mu_{mn}$  as 1, otherwise,  $\mu_{mn}$  is set as 0.

Step 2: Solve the LAC-RCED problem without contingency constraints, according to the value of  $\mu_{mn}$  obtained in Step 1.

Step 3: Calculate the post-contingency power flows and voltage magnitudes in all N-1 and N-2 contingency scenarios by using the proposed LAC-LODF in the LAC model. The termination condition of the procedure is that there are no power flows in any branch and no voltage magnitudes at any bus exceed the limits for all contingencies. If the termination condition is not met, then go to Step 4. If yes, exit the contingency filtering process. This means that a generation dispatch solution satisfying the N-1 and N-2 contingency constraints is found.

Step 4: Screen out the N-1 contingency scenarios that cause the violation of power flow or voltage, and judge if the number of violation scenarios screened is greater than the preset maximum violation scenario (MSV). If yes, sort the violation scenarios in the order of the number of faulty lines, screen the violation scenarios in this queue as evenly distributed as possible, keep the number of screened scenarios at MSV, add these screened scenarios to a violation scenario set which includes all violations screened in each iteration, and then proceed to Step 5. If no, go directly to Step 5.

Step 5: It is worth noting that the adding process of security constraints in Steps 5 and 7 is iterative. That is, the security constraints added by any iteration will remain in the dispatch problem and will be applied to the final dispatch scheme. For the screened N-1 contingency scenarios, add corresponding contingency constraints to LAC-ED and LAC-RCED. Suppose that the

outage of branch  $ij$  causes the power flow violation of branch  $mn$ . To avoid the occurrence of this scenario, the following constraints will be added.

$$(P_{mn}^{L,N-1})^2 + (Q_{mn}^{L,N-1})^2 \leq (S_{mn}^{\max,c})^2 \quad (49)$$

where  $P_{mn}^{L,N-1}$  and  $Q_{mn}^{L,N-1}$  are post-contingency active power and reactive power flow on branch  $mn$  after N-1 outage of branch  $ij$ , and can be expressed as

$$\begin{aligned} P_{mn}^{L,N-1} &= P_{mn}^L + L_{mn,ij}^{P-P} \cdot P_{ij}^L + L_{mn,ij}^{P-Q} \cdot Q_{ij}^L \\ Q_{mn}^{L,N-1} &= Q_{mn}^L + L_{mn,ij}^{Q-P} \cdot P_{ij}^L + L_{mn,ij}^{Q-Q} \cdot Q_{ij}^L \end{aligned} \quad (50)$$

The following is an example of voltage violation, in which the fault of branch  $ij$  causes the voltage violation of bus  $m$ . To avoid the voltage violation in bus  $m$ , the following constraints will be added to LAC-RCED.

$$V_m^{\min} \leq V_m^{N-1} \leq V_m^{\max} \quad (51)$$

where  $V_m^{N-1}$  is the voltage at bus  $m$  after the outage of branch  $ij$ , and can be expressed as follows:

$$V_m^{N-1} = V_m + L_{m,ij}^{V-P} \cdot P_{ij}^L + L_{m,ij}^{V-Q} \cdot Q_{ij}^L \quad (52)$$

Step 6: Screen out the N-2 contingency scenarios that will cause the violation of power flow or voltage. If the number of violated scenarios screened is greater than MVS, the MVS violation scenarios are selected in a similar way to Step 4 and proceed to Step 7. Otherwise, go directly to Step 7.

Step 7: For the N-2 violated scenarios screened out above, add corresponding contingency constraints to LAC-ED and LAC-RCED. Suppose that the outages of branch  $ij$  and  $kl$  cause the power flow violation of branch  $mn$ . To avoid the occurrence of this scenario, the following constraints will be added.

$$(P_{mn}^{L,N-2})^2 + (Q_{mn}^{L,N-2})^2 \leq (S_{mn}^{\max,c})^2 \quad (53)$$

where  $P_{mn}^{L,N-2}$  and  $Q_{mn}^{L,N-2}$  are the post-contingency active power and reactive power flow on branch  $mn$  after N-2 contingency, and can be expressed as

$$\begin{aligned} P_{mn}^{L,N-2} &= P_{mn}^L + L_{mn,lf,kl}^{P-P} \cdot P_{kl}^L + L_{mn,lf,kl}^{P-Q} \cdot Q_{kl}^L + L_{mn,lf,ij}^{P-P} \cdot P_{ij}^L \\ &\quad + L_{mn,lf,ij}^{P-Q} \cdot Q_{ij}^L \\ Q_{mn}^{L,N-2} &= Q_{mn}^L + L_{mn,lf,kl}^{Q-P} \cdot P_{kl}^L + L_{mn,lf,kl}^{Q-Q} \cdot Q_{kl}^L + L_{mn,lf,ij}^{Q-P} \cdot P_{ij}^L \\ &\quad + L_{mn,lf,ij}^{Q-Q} \cdot Q_{ij}^L \end{aligned} \quad (54)$$

Similarly, the outage of branches  $ij$  and  $kl$  causes the voltage violation of bus  $m$ , the following constraints are added to LAC-RCED.

$$V_m^{\min} \leq V_m^{N-2} \leq V_m^{\max} \quad (55)$$

where  $V_m^{N-2}$  is the voltage at bus  $m$  after N-2 contingency, and can be expressed as follows:

$$V_m^{N-2} = V_m + L_{m,lf,kl}^{V-P} \cdot P_{kl}^L + L_{m,lf,kl}^{V-Q} \cdot Q_{kl}^L + L_{m,lf,ij}^{V-P} \cdot P_{ij}^L + L_{m,lf,ij}^{V-Q} \cdot Q_{ij}^L \quad (56)$$

Step 8: Solve the LAC-ED with contingency constraints screened out from Step 4 and Step 6 and set  $\mu_{mn}$  similar to Step 1.

Step 9: According to  $\mu_{mn}$  obtained from Step 8, solve the LAC-RCED with contingency constraints shown in Step 5 and Step 7. Go back to Step 3.

#### 4. Case studies

In this section, several cases are studied to demonstrate the advantages of the model from two perspectives. One is the accuracy of the power flow solution obtained from LAC-LODF in the

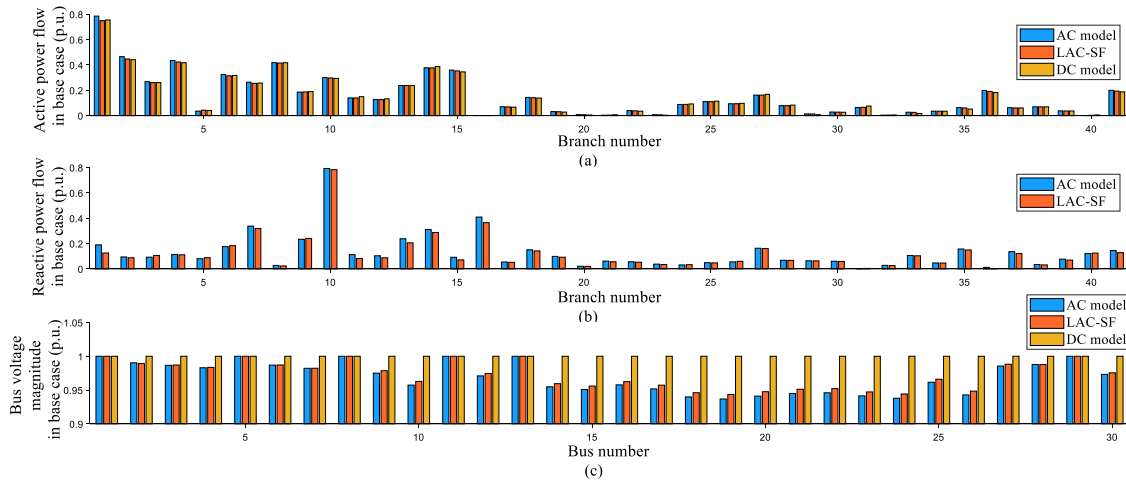


Fig. 4. Comparison of the base case power flow solutions of the AC model, LAC-SF and DC model in a modified IEEE 30-bus system.

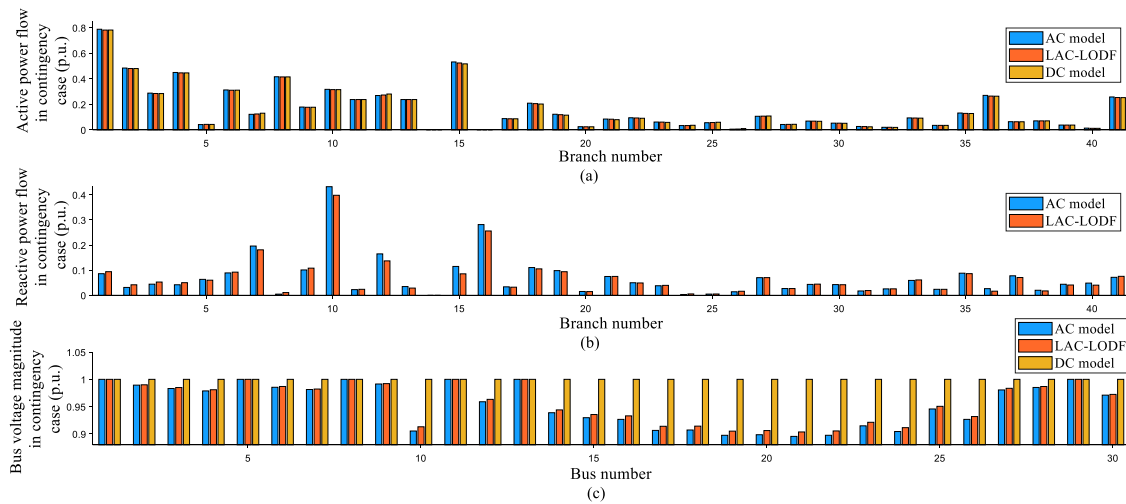


Fig. 5. Comparison of the power flow solutions of contingency case (the outage of branch 14) between the AC model, LAC-LODF and DC model in a modified IEEE 30-bus system.

LAC model, and the other is the effectiveness of the proposed iterative contingency filtering algorithm and LAC-RCED model. Simulations on a modified IEEE 30-bus and the IEEE 118-bus test systems are carried out by using a computer with the MATLAB 2019 platform and Gurobi7.0.1 and IPOPT solvers. In the IEEE 30-bus and 118-bus systems, the reference value of the power flow is 100 MVA. IEEE 30-bus system takes 135 kV as the reference voltage, and the IEEE 118-bus system takes 138 kV instead. More detailed test data are given in Appendix. The designed four cases are as follows:

Case 1: The proposed LAC-SF and LAC-LODF are applied to a modified IEEE 30-bus and the IEEE 118-bus test systems to verify their accuracy for pre-contingency and post-contingency power flow calculation in N-k contingency cases.

Case 2: The proposed LAC-RCED without contingency constraints is studied by comparing it with DC-RCED.

Case 3: LAC-RCED with contingency constraints is studied in the IEEE 30-bus and IEEE 118-bus to investigate the resilience performances of the power dispatch solutions obtained from the model.

Case 4: LAC-RCED with contingency constraints is studied in the more severe failures to demonstrate the resilience of this dispatching strategy.

Three important results are conducted for comparison: active and reactive power flow on a branch and bus voltage magnitude under pre-contingency and post-contingency states. The results of the AC model are set as the benchmark. The equation to calculate the error for the proposed sensitivity factors and the classical DC model is as follows:

$$absolute\_error = |x - x_{AC}|$$

$$relative\_error = \left| \frac{x - x_{AC}}{x_{AC}} \right| \times 100\% \tag{57}$$

where  $x$  is the pre-contingency or post-contingency power flow or bus voltage magnitude calculated by LAC-SF and LAC-LODF or DC model.  $x_{AC}$  is the pre-contingency or post-contingency power flow or bus voltage magnitude calculated by the AC power flow model. To avoid the large relative error caused by branches with negligible power flow, branches with AC power flow values less than 10% of the line capacity are eliminated from statistics in all results of Case 1.

#### 4.1. Case 1

In this case, to show the accuracy of the proposed sensitivity factors, the power flow calculation is performed by fixing the active power and reactive power injections of the PQ buses, active

**Table 2**  
Average and maximum errors of power flow and voltage calculated by LAC-LODF and DC-LODF under N-k failure in a modified IEEE 30-bus system.

Calculation method	Error indicators	N-1	N-2	N-3	N-4
LAC-LODF	Average relative error of active power flow(%)	0.56%	1.01%	1.52%	2.16%
	Average absolute error of active power flow (p.u.)	9.37e-04	0.0019	0.0032	0.0051
	Average relative error of reactive power flow(%)	2.29%	3.44%	5.23%	7.23%
	Average absolute error of reactive power flow (p.u.)	0.0023	0.0037	0.006	0.0091
	Average relative error of node voltage(%)	0.07%	0.17%	0.3%	0.52%
DC-LODF	Average absolute error of node voltage (p.u.)	7.05e-04	0.0016	0.0028	0.0047
	Average relative error of active power flow(%)	0.8%	1.46%	2.06%	2.71%
DC-LODF	Average absolute error of active power flow (p.u.)	0.0012	0.0023	0.0037	0.0055

**Table 3**  
Average and maximum errors of power flow and voltage calculated by LAC-LODF and DC-LODF under N-k failure in a modified IEEE 118-bus system.

Calculation method	Error indicators	N-1	N-2	N-3	N-4
LAC-LODF	Average relative error of active power flow(%)	0.4%	0.74%	1.25%	1.8%
	Average absolute error of active power flow (p.u.)	0.0021	0.0039	0.0066	0.0096
	Average relative error of reactive power flow(%)	0.69%	1.23%	2.03%	2.75%
	Average absolute error of reactive power flow (p.u.)	0.0025	0.0044	0.0073	0.0096
	Average relative error of node voltage(%)	0.0072%	0.0132%	0.0214%	0.0292%
DC-LODF	Average absolute error of node voltage (p.u.)	6.95e-05	1.28e-04	2.07e-04	2.81e-04
	Average relative error of active power flow(%)	0.42%	0.78%	1.3%	1.87%
DC-LODF	Average absolute error of active power flow (p.u.)	0.0022	0.0041	0.0069	0.01

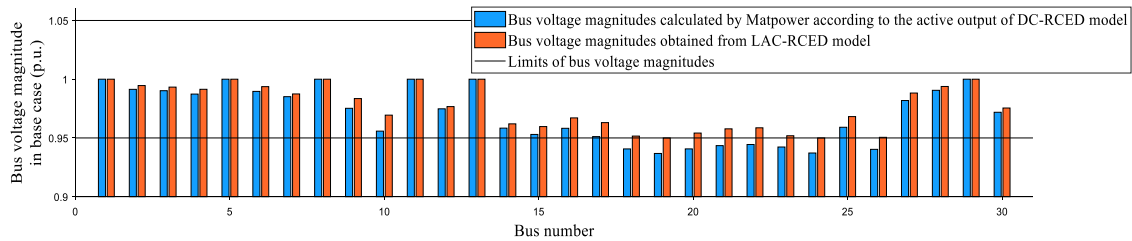


**Fig. 6.** Comparison of the bus voltage magnitudes of the DC-RCED model and LAC-RCED model in a modified IEEE 30-bus system. (For interpretation of the references to color in this figure legend, the reader is referred to the web version of this article.)

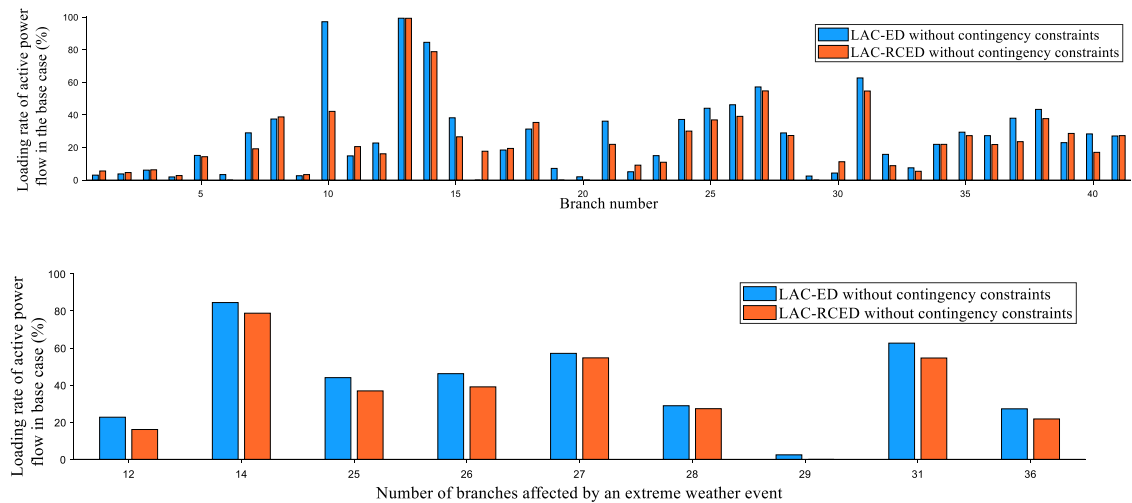


**Fig. 7.** Comparison of the loading rate of active power flow of LAC-ED model and LAC-RCED model in a modified IEEE 30-bus system.

power injections and voltage magnitudes of the PV buses, and voltage angle and magnitude of the slack bus. The LAC-SF and LAC-LODF derived in Section 2 are applied to obtain the pre-contingency and post-contingency power flow solution of the LAC model. The power flow solutions for the AC model and DC model are obtained from MATPOWER 5.1 to make a comparison. The pre-contingency power flow solutions for the above three power flow models are shown in Fig. 4.

Fig. 4(a) and (b) demonstrate the active and reactive power flow on each branch. The bus voltage magnitude profile is shown in Fig. 4(c), in which the bus voltage magnitude in the DC model is assumed to be 1.0 p.u. As shown in Fig. 4(a) and (b), the branch active and reactive power flows in the LAC model calculated by the LAC-SF are very close to those of the AC model. The average relative error of active power flow for all branches is only 1.93% while it is 5.76% in the DC model. The proposed LAC-SF provided a

**Table 4**

Calculation results of the proposed contingency filtering method tested in the IEEE 30-bus system.

Iterations number	Objective	Load shedding percentage	Number of violation scenarios	Number of violation scenarios returned to the master problem	Solution time (s)
0	37 506	0.83%	377	70	2.72
1	75 564	12.22%	3	3	4.97
2	76 798	12.33%	1	1	6.28
3	77 723	12.37%	0	0	7.65

**Table 5**

Calculation results of the contingency filtering method proposed in [32] tested in the IEEE 30-bus system.

Iterations number	Objective	Load shedding percentage	Number of violation scenarios	Number of violation scenarios returned to the master problem	Solution time (s)
0	37 505.72	0.83%	377	3	2.75
1	70 073.61	9.82%	13	3	4.07
2	73 489.61	9.89%	13	3	5.39
3	74 991.79	10.39%	10	3	6.70
4	76 595.72	10.95%	8	3	7.96
5	76 733.72	11.44%	2	2	9.24
6	77 770.58	12.44%	0	0	10.65

**Table 6**

The output of each generator in RCED with/without contingency constraints in a modified IEEE 30-bus system.

Generator number	PG with contingency (p.u.)	QG with contingency (p.u.)	PG without contingency (p.u.)	QG without contingency (p.u.)
1	0.4470	-0.1053	0.1312	0.0478
2	0.7598	0.3049	1.3988	0.1427
3	0.3857	0.2891	0.4891	0.4
4	0.4990	0.0191	0.6451	0.0793
5	0.4660	0.0595	0.1147	0.1666
6	0.1200	0.0157	0.0321	0.0872

**Table 7**

The violated contingency scenarios in LAC-RCED without contingency constraints in a modified IEEE 30-bus system.

N-1 contingency branch	Violated branches or buses after contingency	N-2 contingency branches	Violated branches or buses after contingency
Line 1	Nodes 19, 24, 26	Lines 12, 14	Lines 21, 35 and Nodes 10, 14–26
Line 10	Nodes 18, 19, 23, 24, 26	Lines 12, 25	Nodes 15, 18–20, 23, 24, 26
Line 15	Nodes 18, 19, 23, 24	Lines 25, 36	Line 31 and Nodes 18–20, 23, 24, 26
Line 17	Nodes 14, 18, 19, 23, 24, 26	Lines 27, 28	Lines 30, 31, 35 and Nodes 15, 18, 21–26
Line 35	Nodes 18–26	Lines 31, 36	Lines 30, 32 and Nodes 23–26
The other 103 N-1 violated scenarios are not listed.		The other 200 N-2 violated scenarios are not listed.	

desirable approximation of active power flow. The maximum and average relative errors of reactive power flow in the LAC model are only 15.42% and 6.6%, which is within the acceptable range. Therefore, the proposed  $S^{Q-P}$  and  $S^{Q-Q}$  can provide a desirable approximation calculation of reactive power flow. In terms of bus voltage magnitudes, the accuracy of the LAC model is much higher than that of the classical DC model, as can be seen from Fig. 4(c). The maximum relative error of the LAC model is only 0.71% while it is 6.75% in the DC model. Therefore, the assumption that bus voltage magnitude is equal to 1 is not valid in some cases. Overall, the above results indicate that the proposed LAC-SF can provide a pre-contingency power flow solution where both active and reactive power flow and bus voltage magnitude are notably close to that of the AC model.

Fig. 5 visualizes the post-contingency power flow solution using the outage of branch 14 as an example for illustration.

It can be seen that the post-contingency power flows and voltage magnitudes calculated by the derived LAC-LODF are very close to those of the AC model. The average relative errors of active and reactive power flow in the LAC-LODF model are only 1.19% and 6.43%, while the average relative error of active power flow calculated in the DC model is 2.66% p.u. For bus voltage

magnitude, the maximum relative error of LAC-LODF is 0.91%, which is much lower than the 11.68% calculated in the DC model.

In addition, this paper also compares the accuracy of the proposed N-k LAC-LODF. As shown in Tables 2 and 3, some N-1 to N-4 scenarios will be selected to test the accuracy of the post-contingency power flow and voltage calculated by the LAC-LODF and DC-LODF. Considering that the number of fault combinations is very huge when the total number of combinations is greater than 1000, this experiment will randomly select 1000 scenarios for calculation. It should be noted that even though the scenarios are randomly selected, both LAC-LODF and DC-LODF are compared under the same scenarios. Table 2 shows the average and maximum errors of power flow and voltage under N-k failure in a modified IEEE 30-bus system, and Table 3 shows the indicators in the IEEE 118-bus system.

As shown in Tables 2 and 3, the error calculated by LAC-LODF increases continuously as the severity of faults increases (from N-1 to N-4 faults), but the error in the most severe scenarios is within the acceptable range. In addition, the experimental results also demonstrate the comparison between LAC-LODF and DC-LODF in terms of active power flow accuracy, and LAC-LODF shows the advantage of higher accuracy. Since LAC-LODF takes

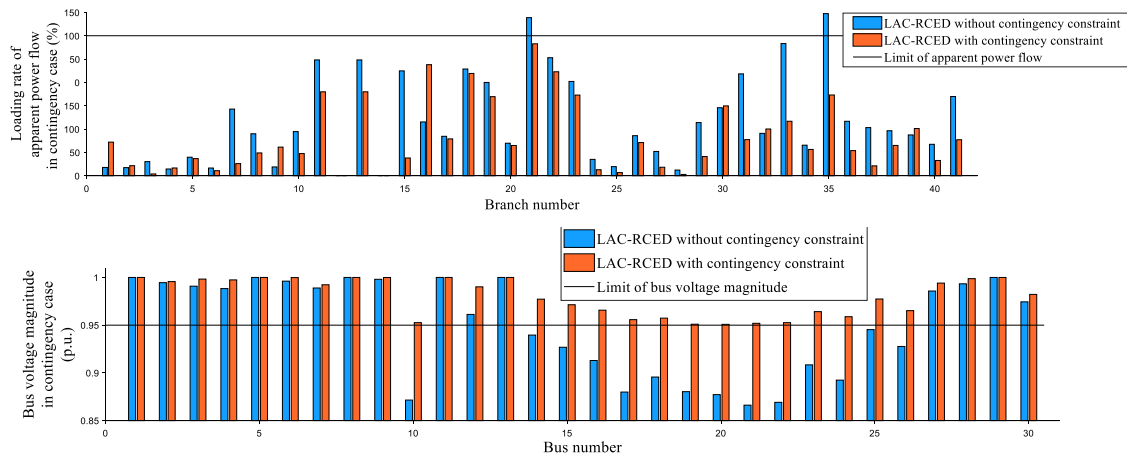


**Fig. 8.** Comparison of the power flow solutions of contingency case (the outage of branches 12 and 14) between the LAC-RCED with/without contingency constraints in a modified IEEE 30-bus system.

**Table 8**  
Calculation results of the proposed contingency filtering method tested in the IEEE 118-bus system.

Iterations number	Objective	Load shedding percentage	Number of violation scenarios	Number of violation scenarios returned to the main problem	Solution time (s)
0	3 105 822	3.75%	184	70	75.62
1	3 854 863	4.79%	14	14	99.62
2	4 092 213	5.1%	0	0	122.79

**Table 9**  
Calculation results of the contingency filtering method proposed in [32] tested in the IEEE 118-bus system.

Iterations number	Objective	Load shedding percentage	Number of violation scenarios	Number of transgression scenarios returned to the main problem	Solution time (s)
0	3 105 822	3.74%	184	4	78.17
1	3 134 032	3.81%	97	4	102.63
2	3 247 476	3.95%	49	4	126.75
3	3 262 244	3.97%	43	4	150.28
4	3 306 185	4.05%	32	3	173.38
5	3 509 964	4.33%	22	3	196.08
6	3 569 147	4.40%	20	3	219.24
7	3 718 010	4.59%	13	3	241.59
8	3 853 556	4.78%	6	3	264.57
9	4 089 888	5.09%	3	3	286.75
10	4 090 026	5.09%	1	2	308.49
11	4 092 215	5.10%	0	0	330.73

reactive power flow into account, LAC-LODF has a closer accuracy in power flow compared to DC-LODF.

4.2. Case 2

In this case, the proposed LAC-RCED without considering the contingency constraints is studied. It is assumed that branches 12, 14, 25–29, 31, and 36 of the IEEE 30-bus system are forecasted to be affected by an extreme weather event. The active power loading rates of these affected branches are optimized in the LAC-RCED to reduce their failure probabilities and avoid power flow transfer once they fail. As mentioned in the introduction, RCED based on the DC model proposed in [10] has a good performance in reducing cascading outages caused by active power transfer, but it cannot take reactive power and voltage magnitude into consideration in the constraints, which may result in the generation dispatch solution obtained by this model violates the bus voltage magnitude limits. Fig. 6 shows the bus voltage magnitudes of the proposed LAC-RCED and the DC-RCED model which is obtained by applying the obtained generation dispatch to the AC power flow calculation in MATPOWER.

As seen from the figure, the voltage magnitudes of buses 18–24 and 26 exceed the limit. Bus voltage magnitudes that are too high or too low will challenge the security operation of the power system, especially in extreme weather conditions, which may result in under-voltage load shedding followed by a blackout. Therefore, the operation limits of bus voltage magnitude should be considered in the resilience-based operation. As can be seen from the red histogram in Fig. 6, the bus voltages of the proposed LAC-RCED are all within the limits. Therefore, the proposed LAC-RCED offers a safer solution compared with DC-RCED.

To verify the effectiveness of the resilience-based objective terms in the LAC-RCED model, the comparison of active power loading rate for all branches and affected branches obtained from LAC-RCED and LAC-ED is shown in Fig. 7.

As demonstrated in Fig. 7, the loading rates of the affected branches in the LAC-RCED model are smaller than those in the LAC-ED model. This validates the effectiveness of the first resilience-based objective term which is proposed to reduce the loading rate of affected lines. Besides, the loading rates for all branches in the LAC-RCED model are also more evenly distributed. These simulation results validate the effectiveness of the

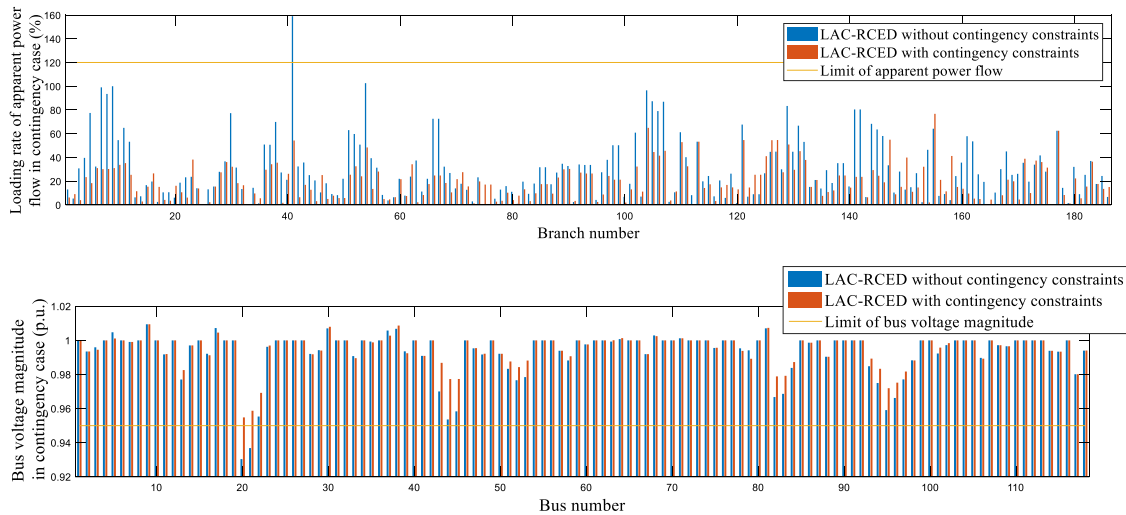


**Fig. 9.** Comparison of the power flow solutions of contingency case (the outage of branches 25 and 33) between the LAC-RCED with/without contingency constraints in the modified IEEE 118-bus system.

**Table 10**  
Results of cascading failure simulations of different models in a modified IEEE 30-bus system.

Models	LAC-RCED	LAC-SCED	LAC-ED
Number of scenarios with overloaded outages in 1000 simulations	176	585	960
Average number of overloaded outage lines in each simulation	0.2250	0.7870	12.7080
Maximum active power load shedding percentage in all simulations	9.5807	16.3541	21.4809
Average active power load shedding percentage in each simulation	0.3693	0.3769	0.8516
Maximum reactive power load shedding percentage in all simulations	8.5286	7.6242	11.1193
Average reactive power load shedding percentage in each simulation	0.0585	0.2839	0.4773

**Table 11**  
Results of cascading failure simulations of different models in a modified IEEE 118-bus system.

Models	LAC-RCED	LAC-SCED	LAC-ED
Number of scenarios with overloaded outages in 1000 simulations	16	18	908
Average number of overloaded outage lines in each scenario	0.04	0.06	5.019
Maximum active power load shedding percentage in all scenarios	2.0468	2.5931	6.8903
Average active power load shedding percentage in each scenario	0.4284	0.4328	1.2920
Maximum reactive power load shedding percentage in all scenarios	2.0492	2.2369	5.3545
Average reactive power load shedding percentage in each scenario	0.6199	0.6364	1.1347

proposed dispatch model in improving the power flow distribution for grid resilience enhancement.

### 4.3. Case 3

In this case, the N-1 contingency constraints for all transmission branches and N-2 contingency constraints for the affected branches are considered in the LAC-RCED with the proposed iterative contingency filtering algorithm. The LAC-RCED model with and without the proposed iterative contingency filtering process is denoted as LAC-RCED with/without contingency constraints in the following discussion.

Firstly, the proposed filtering method is compared with the method presented in [32], where the most severe violation scenario is selected in each iteration based on the degree of violation. Tables 4 and 5 show the calculation results of these two methods tested in the IEEE 30-bus system.

Note that the “solution time” in each iteration is the total time between the start of the solution process and the end of this iteration. As shown in Table 4, the contingency filtering method proposed in this paper takes 3 iterations and 7.65 s to solve the LAC-RCED problem. The number of violations and that of violations returned to the master problem decrease as the iterations increase. As for the contingency filtering method

presented in [32], for each N-1 and N-2 contingency case, the violation scenarios with the greatest violation of power flow and voltage are selected and returned to the master problem. Therefore, the maximum number of violation scenarios returned to the master problem is 4. As seen from Table 5, the number of violation scenarios returned to the master problem in each iteration is 3 or 2, and the method takes 6 iterations and 10.65 s to complete the solution process. Compared to the proposed method, the method proposed in [32] returns fewer violations to the master problem in each iteration and requires more iterations and solution time to solve the LAC-RCED problem. Therefore, the proposed contingency filtering method performs better than the existing method.

Although the LAC-ED without contingency constraints studied in Case 2 could improve the power flow distribution with the help of resilience penalty terms, it cannot ensure secure operation under contingency scenarios. Two kinds of generation dispatch schemes obtained by the LAC-RCED with and without contingency constraints are shown in Table 6. Table 7 shows the violated contingency scenarios in the IEEE 30-bus system of LAC-RCED without contingency constraints. Fig. 8 visualized the detailed power flow solutions of the LAC-RCED model with and without contingency constraints.

**Table A.1**  
The data of branch in the modified 30-bus system.

Branch number	From bus	To bus	Resistance (p.u.)	Reactance (p.u.)	Line charging susceptance (p.u.)	Line capacity (p.u.)
1	1	2	0.0192	0.0575	0.0528	1.30
2	1	3	0.0452	0.1652	0.0408	1.30
3	2	4	0.0570	0.1737	0.0368	0.65
4	3	4	0.0132	0.0379	0.0084	1.30
5	2	5	0.0472	0.1983	0.0418	1.30
6	2	6	0.0581	0.1763	0.0374	0.65
7	4	6	0.0119	0.0414	0.0090	0.90
8	5	7	0.0460	0.1160	0.0204	0.70
9	6	7	0.0267	0.0820	0.0170	1.30
10	6	8	0.0120	0.0420	0.0090	0.32
11	6	9	0	0.2080	0	0.65
12	6	10	0	0.5560	0	0.32
13	9	11	0	0.2080	0	0.65
14	9	10	0	0.1100	0	0.65
15	4	12	0	0.2560	0	0.65
16	12	13	0	0.1400	0	0.65
17	12	14	0.1231	0.2559	0	0.32
18	12	15	0.0662	0.1304	0	0.32
19	12	16	0.0945	0.1987	0	0.32
20	14	15	0.2210	0.1997	0	0.16
21	16	17	0.0524	0.1923	0	0.16
22	15	18	0.1073	0.2185	0	0.16
23	18	19	0.0639	0.1292	0	0.16
24	19	20	0.0340	0.0680	0	0.32
25	10	20	0.0936	0.2090	0	0.32
26	10	17	0.0324	0.0845	0	0.32
27	10	21	0.0348	0.0749	0	0.32
28	10	22	0.0727	0.1499	0	0.32
29	21	22	0.0116	0.0236	0	0.32
30	15	23	0.1000	0.2020	0	0.16
31	22	24	0.1150	0.1790	0	0.16
32	23	24	0.1320	0.2700	0	0.16
33	24	25	0.1885	0.3292	0	0.16
34	25	26	0.2544	0.3800	0	0.16
35	25	27	0.1093	0.2087	0	0.16
36	28	27	0	0.3960	0	0.65
37	27	29	0.2198	0.4153	0	0.16
38	27	30	0.3202	0.6027	0	0.16
39	29	30	0.2399	0.4533	0	0.16
40	8	28	0.0636	0.2000	0.0428	0.32
41	6	28	0.0169	0.0599	0.0130	0.32

**Table A.2**  
The data of bus in the modified 30-bus system.

Bus number	Bus type	Active load (p.u.)	Reactive load (p.u.)
1	Slack	0	0
2	PQ	0.2170	0.1270
3	PQ	0.0240	0.0120
4	PQ	0.0760	0.0160
5	PV	0.9420	0.1900
6	PQ	0	0
7	PQ	0.2280	0.1090
8	PV	0.3000	0.3000
9	PQ	0	0
10	PQ	0.0580	0.0200
11	PV	0	0
12	PQ	0.1120	0.0750
13	PV	0	0
14	PQ	0.0620	0.0160
15	PQ	0.0820	0.0250
16	PQ	0.0350	0.0180
17	PQ	0.0900	0.0580
18	PQ	0.0320	0.0090
19	PQ	0.0950	0.0340
20	PQ	0.0220	0.0070
21	PQ	0.1750	0.1120
22	PQ	0	0
23	PQ	0.0320	0.0160
24	PQ	0.0870	0.0670
25	PQ	0	0
26	PQ	0.0350	0.0230
27	PQ	0	0
28	PQ	0	0
29	PV	0.0240	0.0090
30	PQ	0.1060	0.0190

As shown in Fig. 8, in the LAC-RCED model without contingency constraints, some branches and buses violate the limits. However, in the LAC-RCED model with contingency constraints, the power flows and bus voltage magnitudes are all within the limits. For example, the power flow of branches 21, 35 and voltage magnitude of buses 10, 14–26 will exceed their limits, when branches 12 and 14 fail. It is obvious that with the proposed iterative contingency filtering process, all the violated contingency scenarios listed in Table 7 will be eliminated.

To verify the effectiveness and efficiency of the proposed model in large-scale systems, simulations on a modified IEEE 118-bus system are conducted. In this test system, branches numbered from 20 to 40 are assumed to be affected by an extreme weather event. N-2 contingency constraints for these affected branches and all N-1 contingency constraints are considered in the LAC-RCED with the iterative contingency filtering algorithm. The apparent power flow limits for steady state and contingency states are different. For the safety of power system operation, the steady state operating limit is usually smaller than the contingency state limit. In a contingency state, the power flow on a branch is allowed to exceed the steady-state operating limit for a short time. Therefore, in this case, the apparent power flow limits for contingency cases are set as 120% of the steady state operating limits. Tables 8 and 9 demonstrate the number of violated scenarios and simulation time in each iteration of the iterative contingency filtering process. Hence, the proposed method is suitable for large-scale systems. Fig. 9 shows the power flow solution in terms of apparent power flow and bus voltage

**Table A.3**  
The data of generators in the modified 30-bus system.

Generator number	Generator position	Maximum of active output (p.u.)	Minimum of active output (p.u.)	Maximum of reactive output (p.u.)	Minimum of reactive output (p.u.)	Active output in Case 1 (p.u.)
1	1	3.6020	0	0.1000	-0.2000	1.2571
2	5	1.4000	0	0.5000	-0.4000	1.4000
3	8	1.0000	0	0.4000	-0.4000	0
4	11	1.0000	0	0.4000	-0.4000	0.2376
5	13	1.0000	0	0.2400	-0.4000	0
6	29	1.0000	0	0.2400	-0.4000	0

**Table A.4**  
The data of branch in the modified 118-bus system.

Branch number	From bus	To bus	Resistance (p.u.)	Reactance (p.u.)	Line charging susceptance (p.u.)	Line capacity (p.u.)
1	1	2	0.0303	0.0999	0.0127	1.75
2	1	3	0.0129	0.0424	0.0054	1.75
3	4	5	0.0018	0.0080	0.0011	5.00
4	3	5	0.0241	0.1080	0.0142	1.75
5	5	6	0.0119	0.0540	0.0071	1.75
6	6	7	0.0046	0.0208	0.0028	1.75
7	8	9	0.0024	0.0305	0.5810	5.00
8	8	5	0	0.0267	0	5.00
9	9	10	0.0026	0.0322	0.6150	5.00
10	4	11	0.0209	0.0688	0.0087	1.75
11	5	11	0.0203	0.0682	0.0087	1.75
12	11	12	0.0060	0.0196	0.0025	1.75
13	2	12	0.0187	0.0616	0.0079	1.75
14	3	12	0.0484	0.1600	0.0203	1.75
15	7	12	0.0086	0.0340	0.0044	1.75
16	11	13	0.0223	0.0731	0.0094	1.75
17	12	14	0.0215	0.0707	0.0091	1.75
18	13	15	0.0744	0.2444	0.0313	1.75
19	14	15	0.0595	0.1950	0.0251	1.75
20	12	16	0.0212	0.0834	0.0107	1.75
21	15	17	0.0132	0.0437	0.0222	5.00
22	16	17	0.0454	0.1801	0.0233	1.75
23	17	18	0.0123	0.0505	0.0065	1.75
24	18	19	0.0112	0.0493	0.0057	1.75
25	19	20	0.0252	0.1170	0.0149	1.75
26	15	19	0.0120	0.0394	0.0051	1.75
27	20	21	0.0183	0.0849	0.0108	1.75
28	21	22	0.0209	0.0970	0.0123	1.75
29	22	23	0.0342	0.1590	0.0202	1.75
30	23	24	0.0135	0.0492	0.0249	1.75
31	23	25	0.0156	0.0800	0.0432	5.00
32	26	25	0	0.0382	0	5.00
33	25	27	0.0318	0.1630	0.0882	5.00
34	27	28	0.0191	0.0855	0.0108	1.75
35	28	29	0.0237	0.0943	0.0119	1.75
36	30	17	0	0.0388	0	5.00
37	8	30	0.0043	0.0504	0.2570	1.75
38	26	30	0.0080	0.0860	0.4540	5.00
39	17	31	0.0474	0.1563	0.0200	1.75
40	29	31	0.0108	0.0331	0.0042	1.75
41	23	32	0.0317	0.1153	0.0587	1.40
42	31	32	0.0298	0.0985	0.0126	1.75
43	27	32	0.0229	0.0755	0.0096	1.75
44	15	33	0.0380	0.1244	0.0160	1.75
45	19	34	0.0752	0.2470	0.0316	1.75
46	35	36	0.0022	0.0102	0.0013	1.75
47	35	37	0.0110	0.0497	0.0066	1.75
48	33	37	0.0415	0.1420	0.0183	1.75
49	34	36	0.0087	0.0268	0.0028	1.75
50	34	37	0.0026	0.0094	0.0049	5.00
51	38	37	0	0.0375	0	5.00
52	37	39	0.0321	0.1060	0.0135	1.75
53	37	40	0.0593	0.1680	0.0210	1.75
54	30	38	0.0046	0.0540	0.2110	1.75
55	39	40	0.0184	0.0605	0.0078	1.75
56	40	41	0.0145	0.0487	0.0061	1.75
57	40	42	0.0555	0.1830	0.0233	1.75
58	41	42	0.0410	0.1350	0.0172	1.75
59	43	44	0.0608	0.2454	0.0303	1.75
60	34	43	0.0413	0.1681	0.0211	1.75
61	44	45	0.0224	0.0901	0.0112	1.75
62	45	46	0.0400	0.1356	0.0166	1.75

(continued on next page)

Table A.4 (continued).

Branch number	From bus	To bus	Resistance (p.u.)	Reactance (p.u.)	Line charging susceptance (p.u.)	Line capacity (p.u.)
63	46	47	0.0380	0.1270	0.0158	1.75
64	46	48	0.0601	0.1890	0.0236	1.75
65	47	49	0.0191	0.0625	0.0080	1.75
66	42	49	0.0715	0.3230	0.0430	1.75
67	42	49	0.0715	0.3230	0.0430	1.75
68	45	49	0.0684	0.1860	0.0222	1.75
69	48	49	0.0179	0.0505	0.0063	1.75
70	49	50	0.0267	0.0752	0.0094	1.75
71	49	51	0.0486	0.1370	0.0171	1.75
72	51	52	0.0203	0.0588	0.0070	1.75
73	52	53	0.0405	0.1635	0.0203	1.75
74	53	54	0.0263	0.1220	0.0155	1.75
75	49	54	0.0730	0.2890	0.0369	1.75
76	49	54	0.0869	0.2910	0.0365	1.75
77	54	55	0.0169	0.0707	0.0101	1.75
78	54	56	0.0028	0.0096	0.0037	1.75
79	55	56	0.0049	0.0151	0.0019	1.75
80	56	57	0.0343	0.0966	0.0121	1.75
81	50	57	0.0474	0.1340	0.0166	1.75
82	56	58	0.0343	0.0966	0.0121	1.75
83	51	58	0.0255	0.0719	0.0089	1.75
84	54	59	0.0503	0.2293	0.0299	1.75
85	56	59	0.0825	0.2510	0.0285	1.75
86	56	59	0.0803	0.2390	0.0268	1.75
87	55	59	0.0474	0.2158	0.0282	1.75
88	59	60	0.0317	0.1450	0.0188	1.75
89	59	61	0.0328	0.1500	0.0194	1.75
90	60	61	0.0026	0.0135	0.0073	5.00
91	60	62	0.0123	0.0561	0.0073	1.75
92	61	62	0.0082	0.0376	0.0049	1.75
93	63	59	0	0.0386	0	5.00
94	63	64	0.0017	0.0200	0.1080	5.00
95	64	61	0	0.0268	0	5.00
96	38	65	0.0090	0.0986	0.5230	5.00
97	64	65	0.0027	0.0302	0.1900	5.00
98	49	66	0.0180	0.0919	0.0124	5.00
99	49	66	0.0180	0.0919	0.0124	5.00
100	62	66	0.0482	0.2180	0.0289	1.75
101	62	67	0.0258	0.1170	0.0155	1.75
102	65	66	0	0.0370	0	5.00
103	66	67	0.0224	0.1015	0.0134	1.75
104	65	68	0.0014	0.0160	0.3190	5.00
105	47	69	0.0844	0.2778	0.0355	1.75
106	49	69	0.0985	0.3240	0.0414	1.75
107	68	69	0	0.0370	0	5.00
108	69	70	0.0300	0.1270	0.0610	5.00
109	24	70	0.0022	0.4115	0.0510	1.75
110	70	71	0.0088	0.0355	0.0044	1.75
111	24	72	0.0488	0.1960	0.0244	1.75
112	71	72	0.0446	0.1800	0.0222	1.75
113	71	73	0.0087	0.0454	0.0059	1.75
114	70	74	0.0401	0.1323	0.0168	1.75
115	70	75	0.0428	0.1410	0.0180	1.75
116	69	75	0.0405	0.1220	0.0620	5.00
117	74	75	0.0123	0.0406	0.0052	1.75
118	76	77	0.0444	0.1480	0.0184	1.75
119	69	77	0.0309	0.1010	0.0519	1.75
120	75	77	0.0601	0.1999	0.0249	1.75
121	77	78	0.0038	0.0124	0.0063	1.75
122	78	79	0.0055	0.0244	0.0032	1.75
123	77	80	0.0170	0.0485	0.0236	5.00
124	77	80	0.0294	0.1050	0.0114	5.00
125	79	80	0.0156	0.0704	0.0094	1.75
126	68	81	0.0018	0.0202	0.4040	5.00
127	81	80	0	0.0370	0	5.00
128	77	82	0.0298	0.0853	0.0409	2.00
129	82	83	0.0112	0.0367	0.0190	2.00
130	83	84	0.0625	0.1320	0.0129	1.75
131	83	85	0.0430	0.1480	0.0174	1.75
132	84	85	0.0302	0.0641	0.0062	1.75
133	85	86	0.0350	0.1230	0.0138	5.00
134	86	87	0.0283	0.2074	0.0223	5.00
135	85	88	0.0200	0.1020	0.0138	1.75
136	85	89	0.0239	0.1730	0.0235	1.75
137	88	89	0.0139	0.0712	0.0097	5.00

(continued on next page)

**Table A.4** (continued).

Branch number	From bus	To bus	Resistance (p.u.)	Reactance (p.u.)	Line charging susceptance (p.u.)	Line capacity (p.u.)
138	89	90	0.0518	0.1880	0.0264	5.00
139	89	90	0.0238	0.0997	0.0530	5.00
140	90	91	0.0254	0.0836	0.0107	1.75
141	89	92	0.0099	0.0505	0.0274	5.00
142	89	92	0.0393	0.1581	0.0207	5.00
143	91	92	0.0387	0.1272	0.0163	1.75
144	92	93	0.0258	0.0848	0.0109	1.75
145	92	94	0.0481	0.1580	0.0203	1.75
146	93	94	0.0223	0.0732	0.0094	1.75
147	94	95	0.0132	0.0434	0.0056	1.75
148	80	96	0.0356	0.1820	0.0247	1.75
149	82	96	0.0162	0.0530	0.0272	1.75
150	94	96	0.0269	0.0869	0.0115	1.75
151	80	97	0.0183	0.0934	0.0127	1.75
152	80	98	0.0238	0.1080	0.0143	1.75
153	80	99	0.0454	0.2060	0.0273	2.00
154	92	100	0.0648	0.2950	0.0236	1.75
155	94	100	0.0178	0.0580	0.0302	1.75
156	95	96	0.0171	0.0547	0.0074	1.75
157	96	97	0.0173	0.0885	0.0120	1.75
158	98	100	0.0397	0.1790	0.0238	1.75
159	99	100	0.0180	0.0813	0.0108	1.75
160	100	101	0.0277	0.1262	0.0164	1.75
161	92	102	0.0123	0.0559	0.0073	1.75
162	101	102	0.0246	0.1120	0.0147	1.75
163	100	103	0.0160	0.0525	0.0268	5.00
164	100	104	0.0451	0.2040	0.0271	1.75
165	103	104	0.0466	0.1584	0.0204	1.75
166	103	105	0.0535	0.1625	0.0204	1.75
167	100	106	0.0605	0.2290	0.0310	1.75
168	104	105	0.0099	0.0378	0.0049	1.75
169	105	106	0.0140	0.0547	0.0072	1.75
170	105	107	0.0530	0.1830	0.0236	1.75
171	105	108	0.0261	0.0703	0.0092	1.75
172	106	107	0.0530	0.1830	0.0236	1.75
173	108	109	0.0105	0.0288	0.0038	1.75
174	103	110	0.0391	0.1813	0.0231	1.75
175	109	110	0.0278	0.0762	0.0101	1.75
176	110	111	0.0220	0.0755	0.0100	1.75
177	110	112	0.0247	0.0640	0.0310	1.75
178	17	113	0.0091	0.0301	0.0038	1.75
179	32	113	0.0615	0.2030	0.0259	5.00
180	32	114	0.0135	0.0612	0.0081	1.75
181	27	115	0.0164	0.0741	0.0099	1.75
182	114	115	0.0023	0.0104	0.0014	1.75
183	68	116	0.0003	0.0041	0.0820	5.00
184	12	117	0.0329	0.1400	0.0179	1.75
185	75	118	0.0145	0.0481	0.0060	1.75
186	76	118	0.0164	0.0544	0.0068	1.75

magnitudes. As shown from the figure, all power flows and bus voltage are within their limits. There is no doubt that the solution also ensures that the system is safe for N-2 or N-1 contingency caused by extreme weather because of the contingency filtering process.

As seen from Table 9, the calculation results of the 118-bus system also show that the iterative contingency filtering method proposed in this paper is better than the method proposed in [32], which is similar to the simulation results of the 30-bus system. To sum up, the simulation results of the above three case studies validate the effectiveness of the proposed LAC-RCED and the efficiency of the proposed iterative contingency filtering algorithm.

#### 4.4. Case 4

To investigate the resilience performance of the proposed generation dispatch model, the fast dynamic simulation model for a cascading event presented in [35] is modified to investigate the resilience performances of the power dispatch scheme obtained from different models. The initial first step of the cascading failure simulation procedure was changed to consider the initial trigger

events caused by the extreme weather event, which are generated by Monte Carlo sampling. It is assumed that each line has a probability of outage in the initial state, but the affected lines have a higher probability of failure. In the IEEE 30-bus system, for the lines affected by the extreme weather event, each line has a probability of failure between 60% and 100%, which is randomly generated in each simulation. The rest of the lines have a smaller random failure probability between 0 and 10%. To avoid the initial outages leading to system disconnections, a maximum of two lines are allowed to fail in the initial event. The overloaded outage model considering hidden failure proposed in [36] is used to calculate the failure probability of overloaded lines caused by the power flow transfer after the initial outages. Heavy loading line, that is, loading rate of more than 90%, has a certain probability to be sampled as a fault line. One thousand simulations are performed and the percentage of load shedding is calculated in each simulation to quantify the operational resilience of the power system. Table 10 shows the cascading failure simulation results of the LAC-RCED, LAC-SCED, and LAC-ED models. This experiment selected 1000 simulations to study the variable performance of Table 10. Each simulation means an N-1 or N-2 initial failure and its corresponding cascading failure, in which

**Table A.5**  
The data of bus in the modified 118-bus system.

Bus number	Bus type	Active load (p.u.)	Reactive load (p.u.)
1	Slack	0.765	0.2700
2	PQ	0.3	0.0900
3	PQ	0.585	0.1000
4	PV	0.585	0.1200
5	PQ	0	0
6	PV	0.78	0.2200
7	PQ	0.285	0.0200
8	PV	0.42	0
9	PQ	0	0
10	PV	0	0
11	PQ	1.05	0.2300
12	PV	0.705	0.1000
13	PQ	0.51	0.1600
14	PQ	0.21	0.0100
15	PV	1.35	0.3000
16	PQ	0.375	0.1000
17	PQ	0.165	0.0300
18	PV	0.9	0.3400
19	PV	0.675	0.2500
20	PQ	0.27	0.0300
21	PQ	0.21	0.0800
22	PQ	0.15	0.0500
23	PQ	0.105	0.0300
24	PV	0.195	0
25	PV	0	0
26	PV	0	0
27	PV	1.065	0.1300
28	PQ	0.255	0.0700
29	PQ	0.36	0.0400
30	PQ	0	0
31	PV	0.645	0.2700
32	PV	0.885	0.2300
33	PQ	0.345	0.0900
34	PV	0.885	0.2600
35	PQ	0.495	0.0900
36	PV	0.465	0.1700
37	PQ	0	0
38	PQ	0	0
39	PQ	0.405	0.1100
40	PV	0.99	0.2300
41	PQ	0.555	0.1000
42	PV	1.44	0.2300
43	PQ	0.27	0.0700
44	PQ	0.24	0.0800
45	PQ	0.795	0.2200
46	PV	0.42	0.1000
47	PQ	0.51	0
48	PQ	0.3	0.1100
49	PV	1.305	0.3000
50	PQ	0.255	0.0400
51	PQ	0.255	0.0800
52	PQ	0.27	0.0500
53	PQ	0.345	0.1100
54	PV	1.695	0.3200
55	PV	0.945	0.2200
56	PV	1.26	0.1800
57	PQ	0.18	0.0300
58	PQ	0.18	0.0300
59	PV	4.155	1.1300
60	PQ	1.17	0.0300
61	PV	0	0
62	PV	1.155	0.1400
63	PQ	0	0
64	PQ	0	0
65	PV	0	0
66	PV	0.585	0.1800
67	PQ	0.42	0.0700
68	PQ	0	0
69	PV	0	0
70	PV	0.99	0.2000
71	PQ	0	0

(continued on next page)

**Table A.5** (continued).

Bus number	Bus type	Active load (p.u.)	Reactive load (p.u.)
72	PV	0.18	0
73	PV	0.09	0
74	PV	1.02	0.2700
75	PQ	0.705	0.1100
76	PV	1.02	0.3600
77	PV	0.915	0.2800
78	PQ	1.065	0.2600
79	PQ	0.585	0.3200
80	PV	1.95	0.2600
81	PQ	0	0
82	PQ	0.81	0.2700
83	PQ	0.3	0.1000
84	PQ	0.165	0.0700
85	PV	0.36	0.1500
86	PQ	0.315	0.1000
87	PV	0	0
88	PQ	0.72	0.1000
89	PV	0	0
90	PV	2.445	0.4200
91	PV	0.15	0
92	PV	0.975	0.1000
93	PQ	0.18	0.0700
94	PQ	0.45	0.1600
95	PQ	0.63	0.3100
96	PQ	0.57	0.1500
97	PQ	0.225	0.0900
98	PQ	0.51	0.0800
99	PV	0.63	0
100	PV	0.555	0.1800
101	PQ	0.33	0.1500
102	PQ	0.075	0.0300
103	PV	0.345	0.1600
104	PV	0.57	0.2500
105	PV	0.465	0.2600
106	PQ	0.645	0.1600
107	PV	0.75	0.1200
108	PQ	0.03	0.0100
109	PQ	0.12	0.0300
110	PV	0.585	0.3000
111	PV	0	0
112	PV	1.02	0.1300
113	PV	0.09	0
114	PQ	0.12	0.0300
115	PQ	0.33	0.0700
116	PV	2.76	0
117	PQ	0.3	0.0800
118	PQ	0.495	0.1500

variable performance such as load shedding are assessed. The security constraints considered in the LAC-RCED and LAC-SCED models are the same, while the objectives are different. LAC-ED is the classical economic dispatch problem without contingency constraints and the power flow-related objectives.

As shown in Table 10, the cascading failure simulation result of the LAC-ED model is the worst because no contingency constraint is considered in this model. Comparing the scenarios with overloaded outages in 1000 simulations between LAC-RCED and LAC-SCED models, it can be seen that, in the LAC-RCED model, there are 824 scenarios where the initial outages caused by the extreme event did not trigger a cascading overloaded outage. Moreover, the average number of overloaded outage lines in each scenario of the LAC-RCED model is also less than that of the LAC-SCED model. With fewer overloaded outage scenarios and lines, the amount of load shedding during an extreme event is reduced. The average and maximum percentage of active and reactive power load shedding of the LAC-RCED are all smaller than those of the LAC-SCED model because of the optimization objectives for improving the power flow on the branches. This indicates that large-scale blackouts are reduced in the proposed LAC-RCED model.

**Table A.6**  
The data of generators in the modified 118-bus system.

Generator number	Generator position	Maximum of active output (p.u.)	Minimum of active output (p.u.)	Maximum of reactive output (p.u.)	Minimum of reactive output (p.u.)
1	1	1.00	0	0.15	-0.50
2	4	1.00	0	3.00	-3.00
3	6	1.00	0	0.50	-0.13
4	8	1.00	0	3.00	-3.00
5	10	5.50	0	2.00	-1.47
6	12	1.85	0	1.20	-0.35
7	15	1.00	0	0.30	-0.10
8	18	1.00	0	0.50	-0.16
9	19	1.00	0	0.24	-0.08
10	24	1.00	0	3.00	-3.00
11	25	3.20	0	1.40	-0.47
12	26	4.14	0	10.00	-10.00
13	27	1.00	0	3.00	-3.00
14	31	1.07	0	3.00	-3.00
15	32	1.00	0	0.42	-0.14
16	34	1.00	0	0.24	-0.08
17	36	1.00	0	0.24	-0.08
18	40	1.00	0	3.00	-3.00
19	42	1.00	0	3.00	-3.00
20	46	1.19	0	1.00	-1.00
21	49	3.04	0	2.10	-0.85
22	54	1.48	0	3.00	-3.00
23	55	1.00	0	0.23	-0.08
24	56	1.00	0	0.15	-0.08
25	59	2.55	0	1.80	-0.60
26	61	2.60	0	3.00	-1.00
27	62	1.00	0	0.20	-0.20
28	65	4.91	0	2.00	-0.67
29	66	4.92	0	2.00	-0.67
30	69	8.05	0	3.00	-3.00
31	70	1.00	0	0.32	-0.10
32	72	1.00	0	1.00	-1.00
33	73	1.00	0	1.00	-1.00
34	74	1.00	0	0.09	-0.06
35	76	1.00	0	0.23	-0.08
36	77	1.00	0	0.70	-0.20
37	80	5.77	0	2.80	-1.65
38	85	1.00	0	0.23	-0.08
39	87	1.04	0	10.00	-1.00
40	89	7.07	0	3.00	-2.10
41	90	1.00	0	3.00	-3.00
42	91	1.00	0	1.00	-1.00
43	92	1.00	0	0.09	-0.03
44	99	1.00	0	1.00	-1.00
45	100	3.52	0	1.55	-0.50
46	103	1.40	0	0.40	-0.15
47	104	1.00	0	0.23	-0.08
48	105	1.00	0	0.23	-0.08
49	107	1.00	0	2.00	-2.00
50	110	1.00	0	0.23	-0.08
51	111	1.36	0	10.00	-1.00
52	112	1.00	0	10.00	-1.00
53	113	1.00	0	2.00	-1.00
54	116	1.00	0	10.00	-10.00

In order to broaden the credibility of the experimental results, the above experiments will be carried out in the 118-bus system, and the experimental results are shown [Table 11](#).

With the above experimental results in the 30-bus and 118-bus systems, it can be seen that the proposed generation dispatch model LAC-RCED can provide a more resilient operation with fewer cascading overload outages and less load shedding during extreme events.

## 5. Conclusion and future work

This work conducts a sensitivity analysis of a linearized power flow model with reactive power and voltage magnitude. Three kinds of sensitivity factors, including LAC-SF, LAC-PTDF and LAC-LODF, are derived to calculate the pre-contingency and post-contingency power flow in N-k contingency cases. Based on the

derived LAC-SF and LAC-LODF, a resilience-constrained economic dispatch strategy is developed. This considers the security constraints of N-1 contingency for all lines and N-2 contingency for the affected lines, as well as optimization objectives to improve the power flow distribution in the transmission system. A contingency filtering process is applied to deal with the security constraints of N-1 and N-2 contingency cases in the proposed optimization model. The accuracy of the derived sensitivity factors is verified compared with the power flow solutions obtained from the AC model. Case studies in the IEEE 30-bus show that the derived sensitivity factors could provide a desirable approximation calculation of active and reactive power flow and bus voltage magnitude in the AC model. In addition to this, case studies in the IEEE 30-bus and 118-bus systems also carried out to demonstrate the effectiveness and efficiency performance of the proposed LAC-RCED and contingency filtering algorithm. The

results show that the proposed approach can provide a resilient operation under contingency states. Compared with the existing resilience operation based on the DC model, the proposed model provides a more resilient solution because of the consideration of reactive power and bus voltage magnitude limits. Meanwhile, the calculation performance of the proposed model values its application in practice. Future research will focus on the resilient operation of power systems with high-penetration renewable energy.

### CRedit authorship contribution statement

**Zhaoxiong Huang:** Conceptualization, Methodology, Validation, Writing – original draft. **Liping Huang:** Conceptualization, Methodology, Software, Investigation, Data curation, Formal analysis, Writing – original draft. **Chun Sing Lai:** Conceptualization, Writing – original draft, Data curation, Validation, Resources, Supervision. **Youwei Jia:** Writing – review & editing. **Zhuoli Zhao:** Writing – review & editing. **Xuecong Li:** Writing – review & editing, Project administration. **Loi Lei Lai:** Writing – review & editing, Resources, Project administration, Funding acquisition, Supervision.

### Declaration of competing interest

The authors declare that they have no known competing financial interests or personal relationships that could have appeared to influence the work reported in this paper.

### Data Access Statement

This study is a re-analysis of existing data from MATPOWER (<https://matpower.org>) and modified datasets from MATPOWER are provided in the [Appendix](#) of this paper.

### Acknowledgments

This work was supported by the Education Department of Guangdong Province, China: New and Integrated Energy System Theory and Technology Research Group [Project Number 2016KCXTD022]; National Natural Science Foundation of China (51907031); Brunel University London BRIEF Funding.

### Appendix

The data of the modified 30-bus system includes the data of bus, branch and generator is shown in [Tables A.1–A.3](#), respectively.

The data of the modified 118-bus system includes the data of bus, branch and generator is shown in [Tables A.4–A.6](#), respectively.

### References

- [1] M. Mahzarnia, M.P. Moghaddam, P.T. Baboli, P. Siano, A review of the measures to enhance power systems resilience, *IEEE Syst. J.* 14 (3) (2020) 4059–4070, <http://dx.doi.org/10.1109/JSYST.2020.2965993>.
- [2] A. Pepicciello, A. Vaccaro, L.L. Lai, An interval mathematic-based methodology for reliable resilience analysis of power systems in the presence of data uncertainties, *Energies* 13 (2020) <http://dx.doi.org/10.3390/en13246632>.
- [3] N. Bhusal, M. Abdelmalak, M. Kamruzzaman, M. Benidris, Power system resilience: current practices, challenges, and future directions, *IEEE Access* 8 (2020) 18064–18086, <http://dx.doi.org/10.1109/ACCESS.2020.2968586>.
- [4] R. Eskandarpour, A. Khodaei, J. Lin, Event-driven security-constrained unit commitment with component outage estimation based on machine learning method, in: 2016 North American Power Symposium (NAPS), Denver, CO, USA, 2016, pp. 1–6, <http://dx.doi.org/10.1109/NAPS.2016.7747873>.
- [5] C. Wang, Y. Hou, F. Qiu, S. Lei, K. Liu, Resilience enhancement with sequentially proactive operation strategies, *IEEE Trans. Power Syst.* 32 (4) (2017) 2847–2857, <http://dx.doi.org/10.1109/TPWRS.2016.2622858>.
- [6] K. Lai, Y. Wang, D. Shi, M.S. Illindala, X. Zhang, Z. Wang, A resilient power system operation strategy considering transmission line attacks, *IEEE Access* 6 (2018) 70633–70643, <http://dx.doi.org/10.1109/ACCESS.2018.2875854>.
- [7] G. Huang, J. Wang, C. Chen, C. Guo, Cyber-constrained optimal power flow model for smart grid resilience enhancement, *IEEE Trans. Smart Grid* 10 (5) (2019) 5547–5555, <http://dx.doi.org/10.1109/TSG.2018.2885025>.
- [8] D.N. Trakas, N.D. Hatzigiargyriou, Resilience constrained day-ahead unit commitment under extreme weather events, *IEEE Trans. Power Syst.* 35 (2) (2020) 1242–1253, <http://dx.doi.org/10.1109/TPWRS.2019.2945107>.
- [9] Y.F. Wang, L.P. Huang, M. Shahidehpour, L.L. Lai, H.L. Yuan, F.Y. Xu, Resilience-constrained hourly unit commitment in electricity grids, *IEEE Trans. Power Syst.* 33 (5) (2018) 5604–5614.
- [10] Y.F. Wang, L.P. Huang, M. Shahidehpour, L.L. Lai, Y. Zhou, Impact of cascading and common cause outages on resilience-constrained economic operation of power systems in extreme conditions, *IEEE Trans. Smart Grid* 11 (1) (2019) 590–601.
- [11] C. Guo, Y. Fu, Z.Y. Li, M. Shahidehpour, Direct calculation of line outage distribution factors, *IEEE Trans. Power Syst.* 24 (3) (2009) 1633–1634.
- [12] T. Guler, G. Gross, M.H. Liu, Generalized line outage distribution factors, *IEEE Trans. Power Syst.* 22 (2) (2015) 879–881.
- [13] X. Cheng, T.J. Overbye, PTDF-based power system equivalents, *IEEE Trans. Power Syst.* 20 (4) (2005) 1868–1876.
- [14] S.I. Lim, C.C. Liu, S.J. Lee, M.S. Choi, S.J. Rim, Blocking of zone 3 relays to prevent cascaded events, *IEEE Trans. Power Syst.* 23 (2) (2008) 747–754.
- [15] K.R.C. Mamandur, G.J. Berg, Efficient simulation of line and transformer outages in power systems, *IEEE Trans. Power Appar. Syst. PAS-101* (10) (1982) 3733–3741, <http://dx.doi.org/10.1109/TPAS.1982.317058>.
- [16] Z. Hu, Xifan Wang, A probabilistic load flow method considering branch outages, *IEEE Trans. Power Syst.* 21 (2) (2006) 507–514, <http://dx.doi.org/10.1109/TPWRS.2006.873118>.
- [17] P. Wiest, K. Rudion, A. Probst, Efficient integration of (n-1)-security into probabilistic network expansion planning, *Int. J. Electr. Power Energy Syst.* (ISSN: 0142-0615) 94 (2018) 151–159, <http://dx.doi.org/10.1016/j.ijepes.2017.07.002>.
- [18] R. Yao, F. Qiu, Novel AC distribution factor for efficient outage analysis, *IEEE Trans. Power Syst.* 35 (6) (2020) 4960–4963.
- [19] Z.F. Yang, H.W. Zhong, A. Bose, T.X. Zheng, Q. Xia, C.Q. Kang, A linearized OPF model with reactive power and voltage magnitude: A pathway to improve the MW-only DC OPF, *IEEE Trans. Power Syst.* 33 (2) (2017) 1734–1745.
- [20] D. Shchetinin, T.D.R. Tomas, G. Hug, On the construction of linear approximations of line flow constraints for AC optimal power flow, *IEEE Trans. Power Syst.* 34 (2) (2018) 1182–1192.
- [21] J.W. Yang, N. Zhang, C.Q. Kang, Q. Xia, A state-independent linear power flow model with accurate estimation of voltage magnitude, *IEEE Trans. Power Syst.* 32 (5) (2017) 3607–3617.
- [22] Z.F. Yang, H.W. Zhong, Q. Xia, C.Q. Kang, Solving OPF using linear approximations: Fundamental analysis and numerical demonstration, *IET Gener. Transm. Distrib.* 11 (17) (2017) 4115–4125.
- [23] L.L. Lai, J.T. Ma, R. Yokoyama, M. Zhao, Improved genetic algorithms for optimal power flow under both normal & contingent operation states, *Int. J. Electr. Power Energy Syst.* 19 (5) (1997) 287–292.
- [24] Y.K. Wu, A novel algorithm for ATC calculations and applications in deregulated electricity markets, *Int. J. Electr. Power Energy Syst.* 29 (10) (2007) 810–821.
- [25] H. Yuan, F. Li, Y. Wei, J. Zhu, Novel linearized power flow and linearized OPF models for active distribution networks with application in distribution LMP, *IEEE Trans. Smart Grid* 9 (1) (2018) 438–448.
- [26] R. Habibifar, H. Saber, M.R.K. Gharigh, M. Ehsan, Planning framework for BESSs in microgrids (MGs) using linearized AC power flow approach, in: 2018 Smart Grid Conf. (SGC), Sanandaj, Iran, 2018, pp. 1–7.
- [27] M. Shahidehpour, H. Yamin, Z. Li, Market Operations in Electric Power Systems: Forecasting, Scheduling, and Risk Management, Wiley, New York, NY, USA, 2002.
- [28] J. Alemany, F. Magnago, Benders decomposition applied to security constrained unit commitment: Initialization of the algorithm, *Int. J. Electr. Power Energy Syst.* 66 (2015) 53–66.
- [29] J. Alemany, D. Moitre, F. Magnago, Benders decomposition applied to security constrained unit commitment, *IEEE Latin Amer. Trans.* 11 (1) (2013) 421–425.
- [30] M. Shahidehpour, Y. Fu, Benders decomposition: Applying benders decomposition to power systems, *IEEE Power Energy Mag.* 3 (2) (2005) 20–21.

- [31] D.A. Tejada-Arango, P. Sanchez-Martin, A. Ramos, Security constrained unit commitment using line outage distribution factors, *IEEE Trans. Power Syst.* 33 (1) (2017) 329–337.
- [32] G. Gutiérrez-Alcaraz, N. González-Cabrera, E. Gil, An efficient method for contingency-constrained transmission expansion planning, *Electr. Power Syst. Res.* 182 (2020) 1–11.
- [33] X. Wu, A.J. Conejo, N. Amjady, Robust security constrained ACOPF via conic programming: Identifying the worst contingencies, *IEEE Trans. Power Syst.* 33 (6) (2018) 5884–5891.
- [34] L. Gong, Y. Fu, M. Shahidehpour, et al., A parallel solution for the resilient operation of power systems in geomagnetic storms, *IEEE Trans. Smart Grid* 11 (4) (2020) 3483–3495.
- [35] I. Dobson, B.A. Carreras, V.E. Lynch, An initial model for complex dynamics in electric power system blackouts, in: *Proceedings of the 34th Annual Hawaii International Conference on System Sciences*, IEEE, 2001.
- [36] N.A. Salim, M.M. Othman, I. Musirin, M.S. Serwan, Cascading collapse assessment considering hidden failure, in: *Proceedings of the 1st Int Conf Informatics Comput Intell ICI 2011*, 2011, pp. 318–23.